UNIVERSITY OF BIRMINGHAM
University of Birmingham Research at Birmingham

A small, heterophyllous vine climbing on Psaronius and Cordaites trees in the earliest Permian forests of North China

Pšenička, Josef; Wang, Jun; Hilton, Jason; Zhou, Weiming; Bek, Jiri; Opluštil, Stanislav; Frojdová, Jana

DOI:
10.1086/708814

License:
None: All rights reserved

Document Version
Publisher's PDF, also known as Version of record

Citation for published version (Harvard):
Pšenička, J, Wang, J, Hilton, J, Zhou, W, Bek, J, Opluštil, S & Frojdová, J 2020, 'A small, heterophyllous vine climbing on Psaronius and Cordaites trees in the earliest Permian forests of North China', *International Journal of Plant Sciences*, vol. 181, no. 6, pp. 616–645. https://doi.org/10.1086/708814

Link to publication on Research at Birmingham portal

General rights
Unless a licence is specified above, all rights (including copyright and moral rights) in this document are retained by the authors and/or the copyright holders. The express permission of the copyright holder must be obtained for any use of this material other than for purposes permitted by law.

•Users may freely distribute the URL that is used to identify this publication.
•Users may download and/or print one copy of the publication from the University of Birmingham research portal for the purpose of private study or non-commercial research.
•User may use extracts from the document in line with the concept of 'fair dealing' under the Copyright, Designs and Patents Act 1988 (?)
•Users may not further distribute the material nor use it for the purposes of commercial gain.

Where a licence is displayed above, please note the terms and conditions of the licence govern your use of this document.

When citing, please reference the published version.

Take down policy
While the University of Birmingham exercises care and attention in making items available there are rare occasions when an item has been uploaded in error or has been deemed to be commercially or otherwise sensitive.

If you believe that this is the case for this document, please contact UBIRA@lists.bham.ac.uk providing details and we will remove access to the work immediately and investigate.

Download date: 25. Apr. 2024

Int. J. Plant Sci. 181(6):616–645. 2020.
© 2020 by The University of Chicago. All rights reserved.
1058-5893/2020/18106-0005$15.00 DOI: 10.1086/708814

A SMALL HETEROPHYLLOUS VINE CLIMBING ON *PSARONIUS* AND *CORDAITES* TREES IN THE EARLIEST PERMIAN FORESTS OF NORTH CHINA

Josef Pšenička,[1,*,†,‡] Jun Wang,[2,*,†,§] Jason Hilton,‖ Weiming Zhou,*,† Jiří Bek,# Stanislav Opluštil,** and Jana Votočková Frojdová#

*State Key Laboratory of Palaeobiology and Stratigraphy, Nanjing Institute of Geology and Palaeontology, Chinese Academy of Sciences, No. 39 East Beijing Road, Nanjing 210008, China; †Center for Excellence in Life and Paleoenvironment, Chinese Academy of Sciences, No. 39 East Beijing Road, Nanjing 210008, China; ‡Centrum of Palaeobiodiversity, West Bohemia Museum in Pilsen, Kopeckého sady 2, 301 00 Plzeň, Czech Republic; §University of Chinese Academy of Sciences, No. 19(A) Yuquan Road, Beijing 100049, China; ‖School of Geography, Earth and Environmental Sciences, and Birmingham Institute of Forest Research, University of Birmingham, Edgbaston, Birmingham B15 2TT, United Kingdom; #Department of Paleobiology and Paleoecology, Institute of Geology, Czech Academy of Sciences, Rozvojová 269, 165 00 Praha 6, Czech Republic; and **Faculty of Sciences, Charles University in Prague, Albertov 6, 128 43 Praha 2, Czech Republic

Editor: Stefanie Ickert-Bond

Premise of research. Climbing plants are important components of modern-day tropical forests and primarily comprise angiosperms, but in Paleozoic tropical forests, pteridosperms were the dominant climbers. Climbing pteridosperms are well known from the Paleozoic floras of Euramerica, while much less is known about climbing pteridosperms from other phytogeographic regions. We document from the earliest Permian Taiyuan Formation of Cathaysia a new genus and species of a small vine preserved in situ and in 3D in a volcanic tuff bed from the Wuda locality. We consider the affinity and ecology of the new plant and evaluate its abundance and distribution in the Wuda forest community.

Methodology. Macrofossils were prepared by dégagement, and sharpened needles were used to expose the plant from the overlying sediment. Anatomy was revealed by petrological thin sections. Key features of the plant were observed under scanning electron microscopy.

Pivotal results. Only the aerial organs of the plant are known, and they comprise stems up to 4.5 mm in diameter that bear hooked prickles and fronds. Branching is irregular, probably axillary, with buds situated in axils of the stem and fronds. Stems are eustelic with well-developed secondary xylem. Lanceolate and distinctly asymmetric bipinnate fronds arise from the stem in nodes. Fronds show considerable variation in both size and shape, and pinnules are strongly heterophyllous. Large pinnules have relatively long conical pinnule lobes terminated by pads that are adapted for climbing, which we consider to be pinnule climbing adaptations. Epidermal cells on pinnules have large paracytic stomatal apparatuses. Fertile pinnules with well-developed pinnule laminae appear to have borne reproductive organs above lateral veins and between the midvein and the pinnule margin on the lower (abaxial) pinnule surface. Fertile structures are incompletely preserved and appear to represent pollen organs; seeds are unknown.

Conclusions. Although its fertile organs are unknown, characters of the new plant are most similar to those of the pteridosperm family Callistophytales and in particular *Callistophyton*, but it is distinct from existing genera, leading to the erection of *Wudaeophyton wangii* gen. et sp. nov. *Wudaeophyton wangii* is reconstructed as a vine climbing on *Psaronius* marattialean fern associations in the bottom of the tuff bed and on *Cordaites* gymnosperm associations at the top. We interpret *W. wangii* to most likely be a member of the Callistophytales, leading us to consider the persistence and evolutionary diversification of Callistophytales in the Cathaysian floras after their regional extirpation in Euramerica, which broadly coincided with the onset of the Permian, and their eventual extinction in the Lopingian (upper Permian) before the end-Permian mass extinction event.

Keywords: seed fern, gymnosperm, Callistophytales, *Callistophyton*, *Wudaeophyton*, Cathaysian flora, Euramerican flora, China.

[1] Author for correspondence; email: jpsenicka@zcm.cz.
[2] Author for correspondence; email: jun.wang@nigpas.ac.cn.

Manuscript received October 2019; revised manuscript received January 2020; electronically published June 3, 2020.

Introduction

Climbing plants are important in modern-day tropical forests, where they contribute to diversity, food resources, structural complexity, and plant-animal interactions and ecologically lace

This content downloaded from 147.188.216.059 on July 06, 2020 04:23:42 AM
All use subject to University of Chicago Press Terms and Conditions (http://www.journals.uchicago.edu/t-and-c).

together tree canopies (Burnham 2009). In modern forests, climbers comprise woody lianas and herbaceous vines that are primarily angiosperms (Gentry 1991), occasionally ferns (Smith et al. 2006), and, in one instance, a gymnosperm, with *Gnetum* being the only climbing nonangiosperm seed plant (Burhman 2009). However, during the Paleozoic, a much greater diversity of nonangiosperm seed plants were climbers. Foremost among these were the Paleozoic pteridosperms (seed ferns), which played a role similar to that of angiosperms in terms of their evolutionary adaptations for climbing and their ecological strategies (DiMichele et al. 2006; Burhman 2009). The majority of these climbing pteridosperms are known from the Paleozoic tropical wetlands of Euramerica (e.g., Krings et al. 2003; DiMichele et al. 2006) and include lyginopterids, mariopterids, medullosans, and callistophytaleans. By contrast, remarkably little is known about climbing plants from the Permian tropical wetland floras of Cathaysia. A climbing habit has been interpreted for members of the gigantopterids from the latest Permian of South China (Li et al. 1994; Li and Taylor 1998, 1999), but it remains uncertain whether the gigantopterids are pteridosperms or ferns, as their reproductive organs are unknown. Climbing habits of Cathaysian lyginopterids, mariopterids, medullosans, and callistophytaleans are at present unknown, but considering the floral and ecological relationships of the Permian wetland floras of Cathaysia with those of Euramerica (e.g., Hilton and Cleal 2007), it might be expected that Cathaysia also included a range of climbing pteridosperms.

In the present article, we document the vegetative morphology and anatomy of a new genus and species of vine from the earliest Permian Taiyuan Formation of North China that we interpret to be a member of the Callistophytales. Specimens are preserved as adpressions with 3D and partial anatomical preservation by calcium carbonate within a volcanic ash bed at the Wuda locality (Pfefferkorn and Wang 2007). The intact nature of the specimens allows us to consider frond and pinnule variability on individual plants and also allows us to reconstruct the vegetative organs of the plant on the basis of examples of organic connection between different parts of the same plant. We consider the plant's habit and ecology and integrate this with information from paleoecological assessments that were undertaken when the specimens were collected (Wang et al. 2012) in order to enable an evaluation of the abundance and distribution of the new plant within the flora.

Geological Information

Specimens were collected during paleobotanical excavations in 2011 and 2017 in the Hongqi Coal Mine within the Wuda coalfield (Wuda coal district, Inner Mongolia, China; fig. 1) by a collaborative Chinese and Czech research team. The exceptionally well-preserved fossil plant remains documented are preserved in situ in a volcanic ashfall tuff that occurs between coal seams number 6 and number 7 in the uppermost part of the Taiyuan Formation (Pfefferkorn and Wang 2007). The tuff flora represents a T^0 assemblage (Wang et al. 2012) with synchronous ashfall deposition across the coal basin. Volcanic ash smothered growing plants in situ within the peat-forming swamp, creating an obrution event and a remarkable terrestrial *konservat lagerstätte* (Wang et al. 2012). Fossils present are often entire, with their morphology preserved, and in many cases their anatomy is also preserved in some parts of the plant. The present fossils represent sections of entire plants, but none are complete (see "Discussion" for further information).

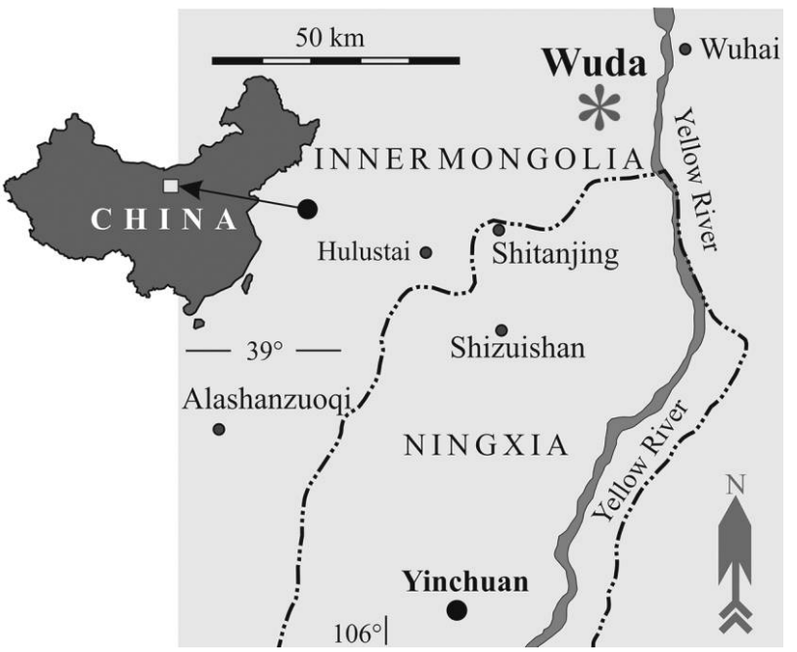

Fig. 1 Outline map of China showing position of the collection locality for *Wudaeophyton wangii* gen. et sp. nov. in the Wuda coal mine, Inner Mongolia, China. A color version of this figure is available online.

This content downloaded from 147.188.216.059 on July 06, 2020 04:23:42 AM
All use subject to University of Chicago Press Terms and Conditions (http://www.journals.uchicago.edu/t-and-c).

Distribution of specimens of the new plant within the tuff profile is shown in figure 2. They are present only in the middle and upper layers of the tuff horizon and are most abundant at 40–50 cm above the number 7 coal seam, where slightly more than 40% of the specimens occur. In the ash, the new plant occurs in association with the marattialean tree fern *Psaronius* in the middle unit of the tuff, but in the upper tuff unit, it is associated with the cordaitalean gymnosperm *Cordaites* (fig. 2).

Despite exhaustive and systematic collecting from the tuff horizon (Pfefferkorn and Wang 2007; Opluštil et al., forthcoming), only 64 specimens of the present species have been discovered in the ca. 2000-m^2 area examined by paleoecological surveying. The present account is based on the 20 most complete and best-preserved specimens (PB23025–PB23044); the remaining specimens provided no additional insights.

Stratigraphically, the Wuda tuff horizon has been dated to the latest Carboniferous or earliest Permian using plant fossil biostratigraphy (Wang and Pfefferkorn 2013). Recent high-precision radiometric dating of zircon crystals in the plant-bearing tuff horizon provides an age of 298.34 ± 0.09 Ma (Cohen et al. 2013), placing it in the lowermost part of the earliest Permian Asselian stage.

Material, Methods, and Terminology

Specimens (PB23025–PB23044) are preserved as adpressions with 3D preservation, with axes of the plant also having occasional cellular preservation by permineralization in calcium carbonate (see Wang et al. 2009). Cuticles are not preserved, but imprints of epidermal features may be present as impressions in the fine-grained tuff.

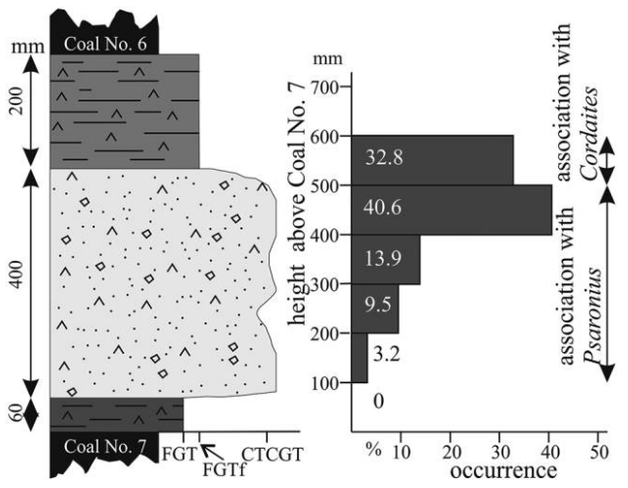

Fig. 2 Idealized vertical section through the geological succession between coal seams number 6 and number 7 in the Wuda coalfield, showing the occurrence and frequency of specimens of *Wudaeophyton wangii* gen. et sp. nov. The volcanic tuff layer consists of a lower 600-mm-thick layer that consists of white, light gray, and bluish-colored layered ash; a middle 400-mm-thick layer that consists of white coarse-grained crystalline tuff; and an upper 200-mm-thick layer that consists of light gray fine-grained ash. Thickness of tuff layers is slightly variable. FGT = fine-grained tuff; FGTf = fine-grained tuffite; CTCGT = coarse-grained crystal tuff. A color version of this figure is available online.

Megafossils were prepared by dégagement (Fairon-Demaret et al. 1999), and either sharpened needles or mechanical excavators were used to remove sediment overlying the plant fossils. Macrophotography was achieved using a Canon G5 X digital camera. Anatomically preserved stems were prepared as petrological thin sections. Stems were mechanically separated from the surrounding matrix and were embedded in epoxy resin. Once set, resin blocks were cut and polished using a Discoplan TS (Centrum of Palaeobiodiversity, West Bohemia Museum in Pilsen, Czech Republic) before being mounted on glass slides with a coverslip. Microscope slides were observed and photographed under dissecting microscopes (Olympus SZX12 and Zeiss Axio Zoom.V16) and compound optical microscopes (Olympus BX51 and Zeiss Axio Imager.Z2).

Imprints of cuticular features in the ash were observed directly under scanning electron microscopy (SEM) for observation of rachial, tendril, and epidermal structures. Some specimens revealed results when uncoated, while others required gold coating before SEM analysis. SEM analysis was undertaken using a JEOL 6380LV at the Institute of Geology and Paleontology, Faculty of Sciences, Charles University in Prague, and a Tescan VEGA3 XMU at the State Key Laboratory of Palaeobiology and Stratigraphy, Nanjing Institute of Geology and Palaeontology, Chinese Academy of Sciences, Nanjing, China.

All specimens are deposited in the collections of the State Key Laboratory of Palaeobiology and Geology, Nanjing Institute of Geology and Palaeontology.

We used standard terminology for the description of morphological and anatomical features of the studied plant, as summarized in figure 3. We also define specialized climbing structures that occur on modified pinnules and establish the term "pinnule climbing adaptations"; the name is derived from their presumed function and their position on modified pinnules, where they comprise linear lobes terminated by swollen structures.

Systematic Paleontology

Order—Incertae Sedis

Family—Incertae Sedis

Genus—Wudaeophyton *gen. nov. J. Pšeničkа and J. Wang*

Species—Wudaeophyton wangii *sp. nov. J. Pšeničkа and J. Wang*

Combined generic and specific diagnosis. Plant with slender stems producing pinnately compound fronds/leaves and axillary buds or branches, with irregularly spaced small hooked prickles on surface. Stem eustelic with up to eight primary xylem strands, including five axial mesarch primary xylem bundles and two to three leaf traces surrounding the pith. Leaf traces with double vascular strand at leaf bases. Cortex comprising cells with secondary thickenings and secretory cells. Secondary xylem with large tracheids and narrow rays. Fronds/leaves bipinnately compound, 50–250 mm long, with undivided petiole. Small fronds/leaves with only entire-margined pinnules. Larger fronds/leaves with laminate pinnules proximally and lobate and bilobate

This content downloaded from 147.188.216.059 on July 06, 2020 04:23:42 AM
All use subject to University of Chicago Press Terms and Conditions (http://www.journals.uchicago.edu/t-and-c).

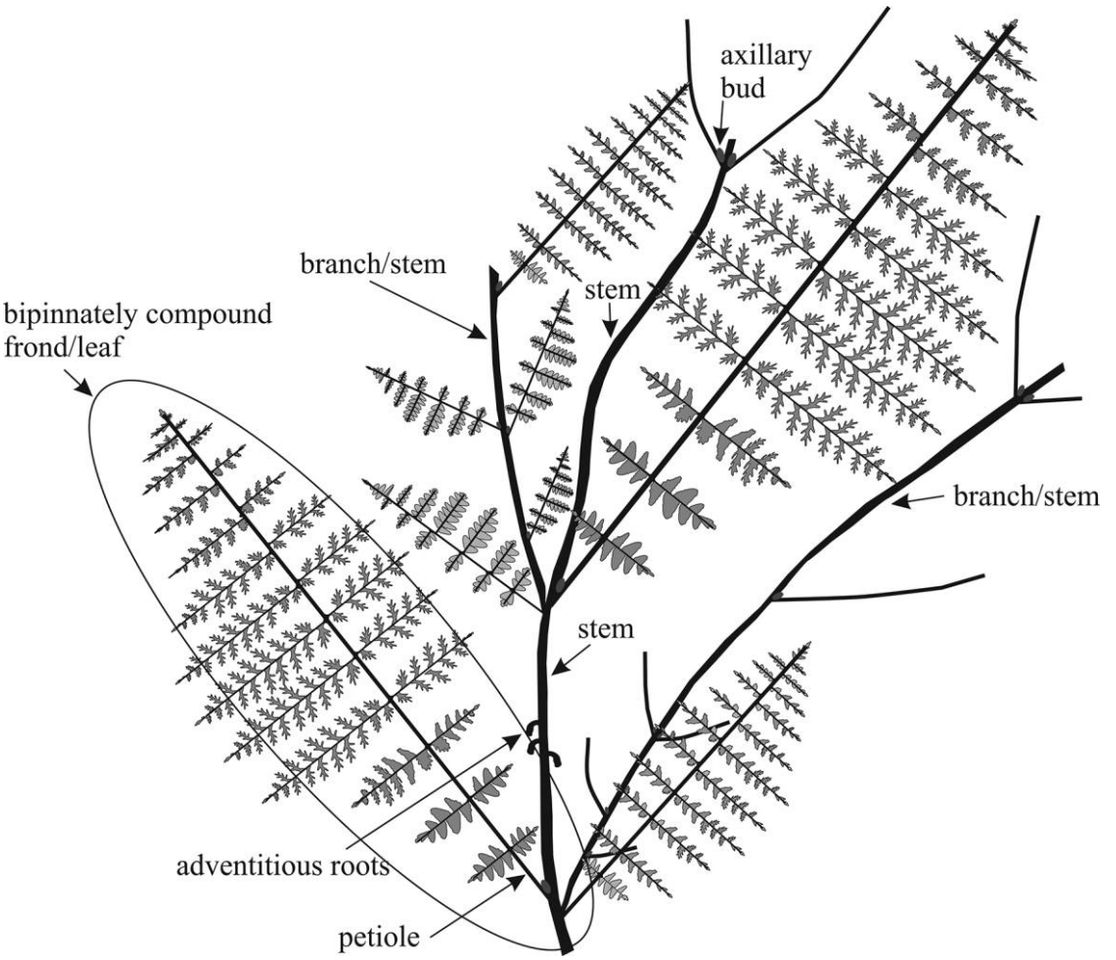

Fig. 3 Diagrammatic representation of the terminology used to describe features of *Wudaeophyton wangii* gen. et sp. nov.

pinnules with reduced pinnule lamina medially and distally. Small triangular to tongue-shaped pinnules situated in departure point of ultimate rachis from frond rachis. Pinnules heterophyllous, slightly asymmetric, varying from entire margined with fully developed pinnule lamina to lobate with partly developed pinnule lamina to deeply lobate with distinctly reduced lamina. Pinnules lacking a lamina with pinnule climbing adaptations. Lateral veins dichotomizing once, rarely twice. Stomata paracytic with two subsidiary cells.

Etymology. The new genus is named after the town of Wuda, which is near the Hongqi Coal Mine collecting locality. The specific epithet is in honor of Professor Wang Shi-Jun in recognition of his prolific, pioneering, and detailed systematic investigations of anatomically preserved plants from China.

Remarks. The genus *Callistophyton* is based on anatomically preserved stems for which it is problematic to assign specimens with other kinds of preservation to the genus. Rothwell (1981) presented permineralized specimens of *Callistophyton* with well-preserved morphological outlines and venation of pinnules as *C. boyssetii*. While the anatomy of the specimens described here shows great similarity to *Callistophyton*, key diagnostic characters of *Callistophyton*, including cellular features of the pith, most parts of the cortex, the secondary phloem, and reproductive organs, are unclear or have not been observed in the present specimens. This problem is further exacerbated by the mode of preservation of the present specimens, which are mostly preserved as adpressions with morphological rather than anatomical characters evident, in contrast to the anatomically preserved specimens of *Callistophyton*. Furthermore, pinnule morphology in the Wuda plant is very different from that of species of *Callistophyton*, which broadly conform to species of the adpression fossils *Dicksonites* and *Pseudomariopteris* (see below). Consequently, it is not possible to place the present species within *Callistophyton* despite its overall vegetative similarity to that genus. Differences from all previously recognized Callistophytales justify the creation of *W. wangii* gen. et sp. nov. Although we formally designate *W. wangii* as incertae sedis because its fertile organs are unknown, the similarity of the vegetative organs to those of *Callistophyton* is compelling and suggests that it is a callistophytalean pteridosperm. Finally, as the genus *Wudaeophyton* is at present monotypic, we have created a combined generic and specific diagnosis because it is not possible to separate generically diagnostic characters from those that would be diagnostic of different species.

This content downloaded from 147.188.216.059 on July 06, 2020 04:23:42 AM
All use subject to University of Chicago Press Terms and Conditions (http://www.journals.uchicago.edu/t-and-c).

Holotype. PB23025 (fig. 4*A*).

Paratypes. PB23027 (well-preserved stelar anatomy with branching; fig. 5*C*) and PB23044 (fertile pinnules; fig. 10*A*).

Type locality. Hongqi Coal Mine, Wuda, Inner Mongolia (lat. 39°29′13.8″N, long. 106°39′00.0″E).

Horizon. Wuda ash bed, between coal seams number 6 and number 7, Taiyuan Formation.

Stratigraphic age. Earliest Asselian (Permian).

Depository. Nanjing Institute of Geology and Palaeontology, Chinese Academy of Sciences.

Description

Gross Morphology

This species has stems and fronds/leaves that are typically found in organic connection to one another and that show the organization and gross morphology of the plant (figs. 4–7). Stems are slender (fig. 4), and compound fronds/leaves (fig. 7) are bipinnate, with simple petioles lacking dichotomies. Branching is probably by axillary buds or branches (figs. 5, 6), and petioles depart irregularly from nodes arranged with short (a few millimeters) or long (more than 200 mm) internodes. Pinnules (figs. 8–10) are strongly heterophyllous and vary considerably in their morphology, from being entire margined with fully developed pinnule laminae to having partly developed pinnule laminae to having deeply lobate pinnules with highly reduced laminae (fig. 8). Many pinnules have specialist adaptations for a climbing habit (see below; fig. 11). Although incompletely preserved, fertile pinnules have fully developed pinnule laminae that bear small scars on the abaxial surface where reproductive organs appear to have been embedded (fig. 12). Preserved epidermal features show stomata to be paracytic (figs. 13, 14). Anatomically (figs. 15–17), stems are eustelic with a central pith surrounded by mesarch primary xylem bundles and a thin zone of secondary xylem, with the cortex including secretory cells.

Stem Morphology

Stems are generally straight and vary from 2.5 to 4.5 mm wide. Branching of the stem is preserved only in the holotype (PB23025) and the paratype (PB23027). The holotype (fig. 4*A*) has two stems (fig. 4*B*, I and I**); stem I is 3 mm wide, while stem I** is slightly narrower and 2.5 mm wide. The slender stem, I**, most probably (real connection is missing in the holotype slab) originates from a slightly swollen node situated on the lower part of the rock slab (arrow in fig. 4*B*). In this part, two nodes are probably presented (see below; fig. 4*B*), although the nodal zone is not well preserved (fig. 5*A*). It appears that the petioles (fig. 5*B*, II) and branch (fig. 5*B*, I**) arise from the node, with the stem continuing (fig. 5*B*, I) distally after branching. Nevertheless, the I** is preserved only as remains of coal film between petiole II and stem I, and therefore this situation is not clear (fig. 5*A*, 5*B*). Petiole II, situated on the right side in figure 5*B*, seems to depart from the same node as the branch I**. Nevertheless, it is not possible to determine the precise point of departure of petioles II situated on both sides of stem I in figure 5*B* because of poor preservation (fig. 5*A*). Stem I** from figure 5*B* represents the same stem figured in figure 4*B* I**, although ca. 20 mm of the stem is missing because of incomplete preservation.

Specimen PB23027 shows the stem branching in what appears to be a dichotomous fashion in the upper part of figure 6*A*. However, one of the axes (fig. 6*A*, I) is 3 mm wide and is the same as the stem below the level of the branching, while the other axis (fig. 6*A*, I*) is slightly narrower and is 2.6 mm wide, suggesting unequal and not dichotomous branching. The departing branch (fig. 6*A*, I*) arises in the axil of the stem and a petiole departure, where the petiole is represented by a very short frond rachis situated under the branch (arrow, fig. 6*C*), and a leaf is absent. Therefore, in this case the branching appears to be rather axillary and not dichotomous. Although this latter stem is isolated from other parts of the plant and lacks attachment to fronds/leaves to allow it to be identified on the basis of its morphology, its anatomy corresponds with that of the holotype (see below), and the stem is associated with fronds/leaves bearing pinnules characteristic of the species (fig. 6*A*).

Only a single bud is present in the studied specimens and occurs on the holotype. The bud is 1.5 mm long and 0.8 mm wide and is positioned on the stem in the axil of a petiole (arrowhead in fig. 5*D*). The petiole is small and enters into small frond/leaf-bearing pinnules with fully developed pinnule laminae (fig. 6*C*).

On the stem, prickles are infrequent. They are oriented with their long axes toward the proximal part of the plant and are inserted into the stem at an angle of ca. 54°–80° (arrows in fig. 5*E*). Individual prickles are 0.3–0.4 mm long and 0.4 mm wide at their base, with tips typically hooked. The same type of prickles, but smaller, occurs on frond rachises.

Frond/Leaf

Bipinnate fronds of different sizes are attached to the stem at nodes. Both the holotype PB23025 (fig. 4*A*) and the specimen in figure 7*F*, 7*G* show two petioles arising from the stem nodal zone, but from these specimens it is unclear whether they depart at the same level or whether they arise from two closely spaced departures. In other cases coming from the holotype slab (fig. 5*D*) and specimen PB23027 (figs. 6*B*, 5*C*, arrow), only a single petiole departs from the stem. Rachises (including fronds and ultimate rachises) are mostly oriented alongside stems (e.g., fig. 4), which appears to be taphonomic and is associated with preburial pendulous organs positioning into a single plane within the ash deposit. The frequency of petiole departures from the stem is variable. In the thickest stems (fig. 4*B*) from an approximately 260-mm-long section, two nodes are typically present in one nodal zone, and the two nodes seem to occur millimeters apart from each other. By contrast, petioles attached to the proximal part of a departing branch in the holotype slab show two nodes spaced ca. 13 mm apart from each other (fig. 4*B*, stem I**). Figure 5*C* clearly shows two attached petioles (arrows) and one probable node (arrowhead). Thus, nodal distances can vary considerably; they can be short steps of ca. 13–20 mm apart on the proximal parts of branches, while nodes on the widest stems created nodal zones with individual nodes situated millimeters apart but with longer internodal zones of 200 mm or more between nodal zones. Poor preservation limits more precise measurements.

Fronds vary in size depending on their position on the plant, function, and stage of ontogenetic development. The largest fronds are ca. 200 mm long, as seen in the holotype. Specimen PB23032 illustrates the middle part of a large frond and has a 1.5-mm-wide frond rachis, long ultimate pinnae (>40 mm)

This content downloaded from 147.188.216.059 on July 06, 2020 04:23:42 AM
All use subject to University of Chicago Press Terms and Conditions (http://www.journals.uchicago.edu/t-and-c).

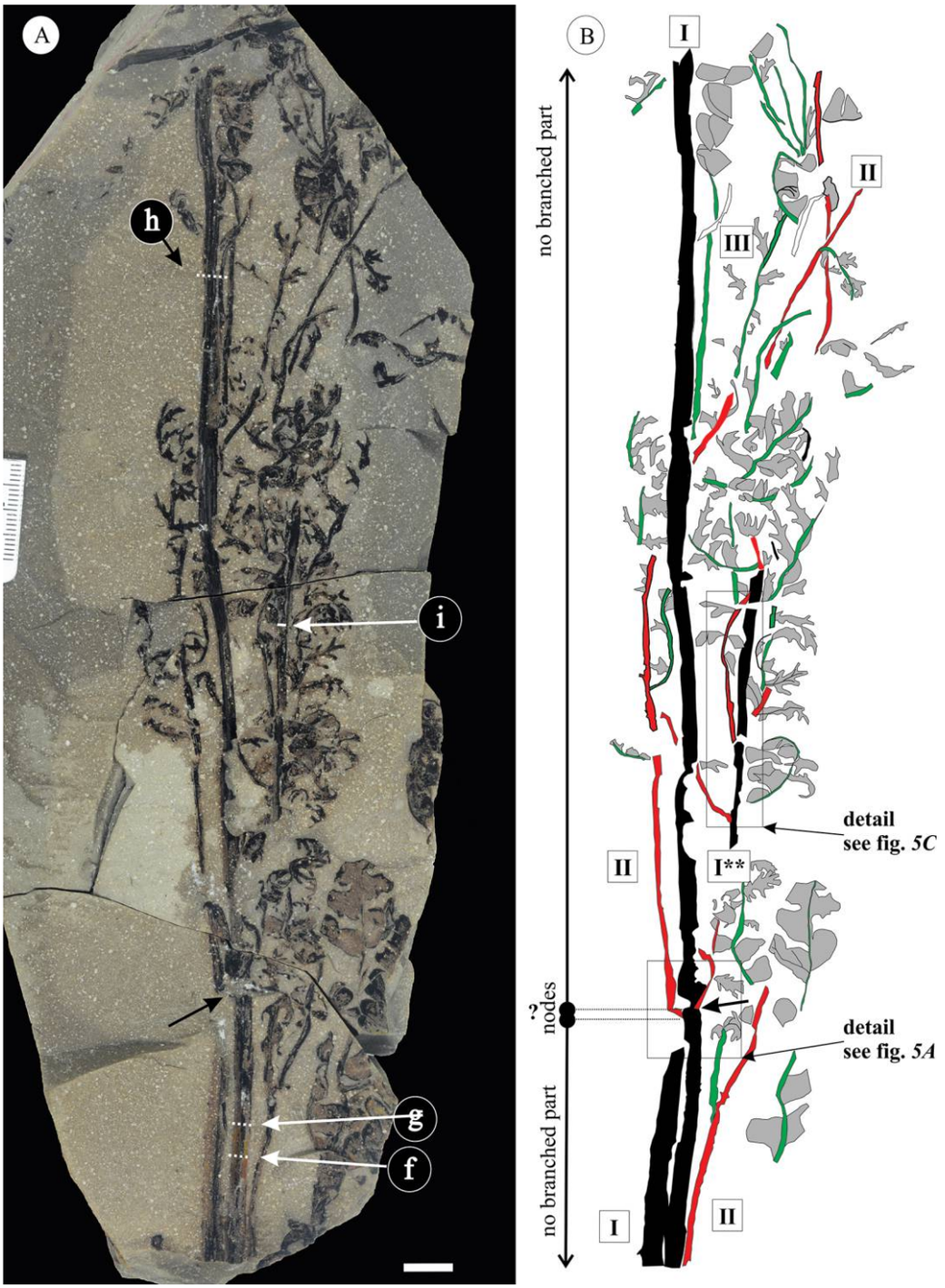

Fig. 4 Holotype PB23025 of *Wudaeophyton wangii* gen. et sp. nov. *A*, Holotype slab. Labels f–i indicate positions of sampled anatomical sections, and the arrow shows position of the nodal zone, probably with two nodes. Scale bar = 10 mm. *B*, Camera lucida drawing of the holotype slab from *A*. Black rachises indicate the stem, red rachises indicate the frond/primary rachis, and green rachises indicate the ultimate rachises. Arrow shows the nodal zone; gray fields represent the occurrence of pinnules with fully developed pinnule laminae. I = stem; I** = branch/stem; II = frond/primary rachis; III = ultimate rachis. Scale bar = 10 mm.

This content downloaded from 147.188.216.059 on July 06, 2020 04:23:42 AM
All use subject to University of Chicago Press Terms and Conditions (http://www.journals.uchicago.edu/t-and-c).

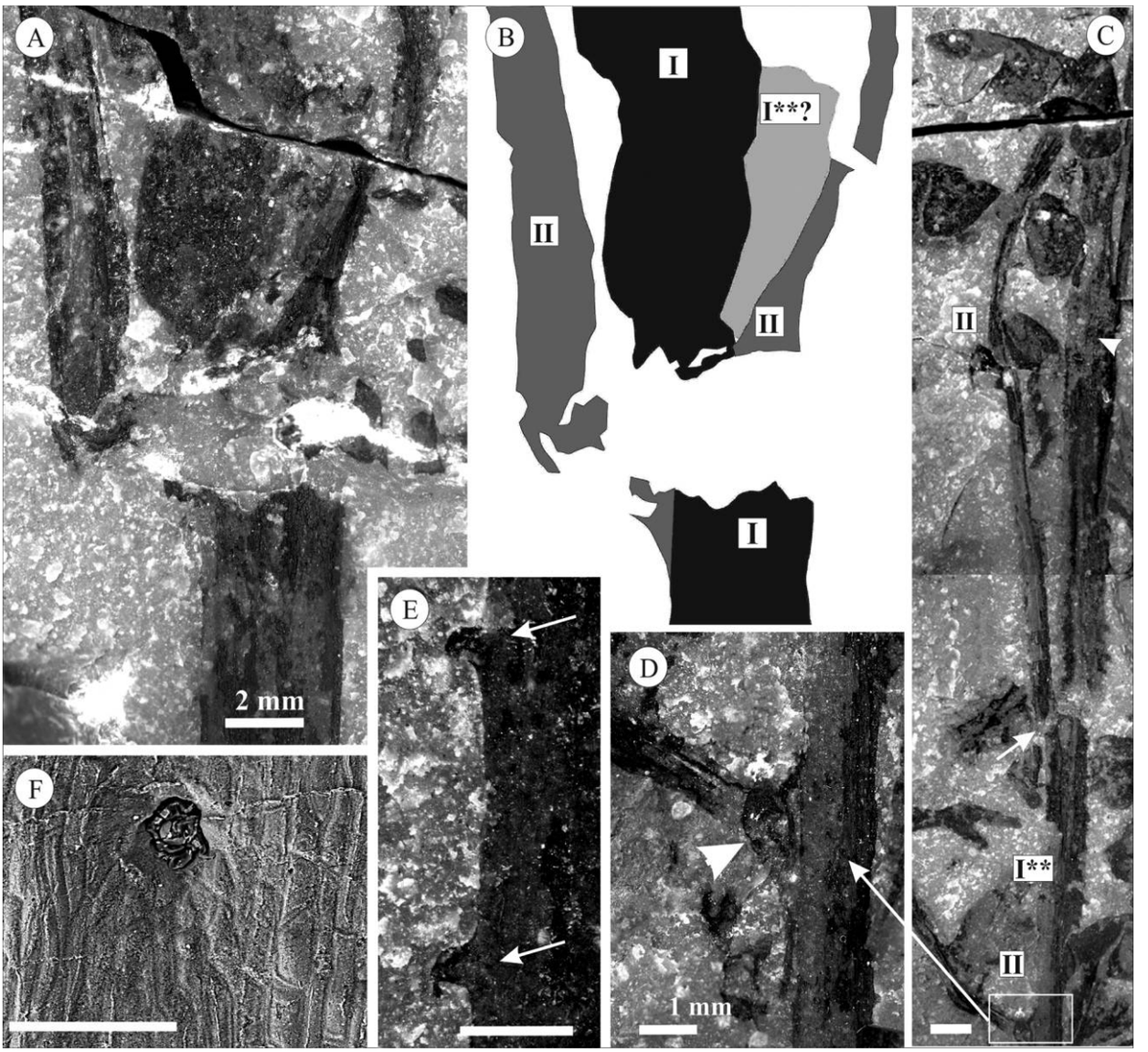

Fig. 5 Details of the holotype (PB23025) of *Wudaeophyton wangii* gen. et sp. nov. *A*, *B*, Nodal zone on the stem with two petioles (II) and a branch (I**) outgoing from probably two nodes on stem (I). Scale bar = 2 mm. *C*, Proximal part of branched stem (I**) with two attached petioles (II; arrows) and another disputable node with a small leaf scar (arrowhead). One petiole is entering into well-preserved frond/leaf bearing short ultimate rachises with laminate pinnules. Rectangle represents the part figured in *D*. Scale bar = 2 mm. *D*, Petiole outgoing from a node with bud (arrowhead) situated in axil of petiole and stem. Detail from *C*. Scale bar = 1 mm. *E*, Hooked cortical prickles (arrows) from stem I. Scale bar = 1 mm. *F*, Spine base on the frond rachis, with drop-shaped base in tangential view. SEM. Scale bar = 150 μm. A color version of this figure is available online.

bearing large pinnules with reduced pinnule laminae, and well-developed pinnule lobes (fig. 7*D*, 7*E*). Some specimens show fronds with a distinctive asymmetry where the ultimate pinnae on one side are shorter than the ultimate pinnae on the opposite side (fig. 6*D*). However, the overall frond shape is not readily identifiable, as nearly all ultimate pinnae, which define the outline of the frond, are incompletely preserved. Distal parts of large fronds/leaves also show this distinctive asymmetry and consist of significantly lobate pinnules (fig. 6*E*). Short ultimate pinnae bearing pinnules with well-developed pinnule laminae are situated in the lower part of the leaf (figs. 9*E*, 10*D*). Ultimate pinnae in these cases are very short (ca. 15–20 mm).

Medium-size fronds are ca. 120–150 mm long (fig. 7*A*, 7*B*) and mostly bear pinnules with developed pinnule laminae and marginal lobes (fig. 9*A*). Specimen PB23026 is a nearly complete frond of this type (fig. 7*A*, 7*B*) and is lanceolate in outline. Ultimate pinnae are subopposite, with the distance between the two opposite ultimate pinnae increasing apically. The frond was most likely asymmetric (fig. 7*A*, 7*B*), as the incomplete ultimate pinnae on the left side are the same length as complete pinnae on

This content downloaded from 147.188.216.059 on July 06, 2020 04:23:42 AM
All use subject to University of Chicago Press Terms and Conditions (http://www.journals.uchicago.edu/t-and-c).

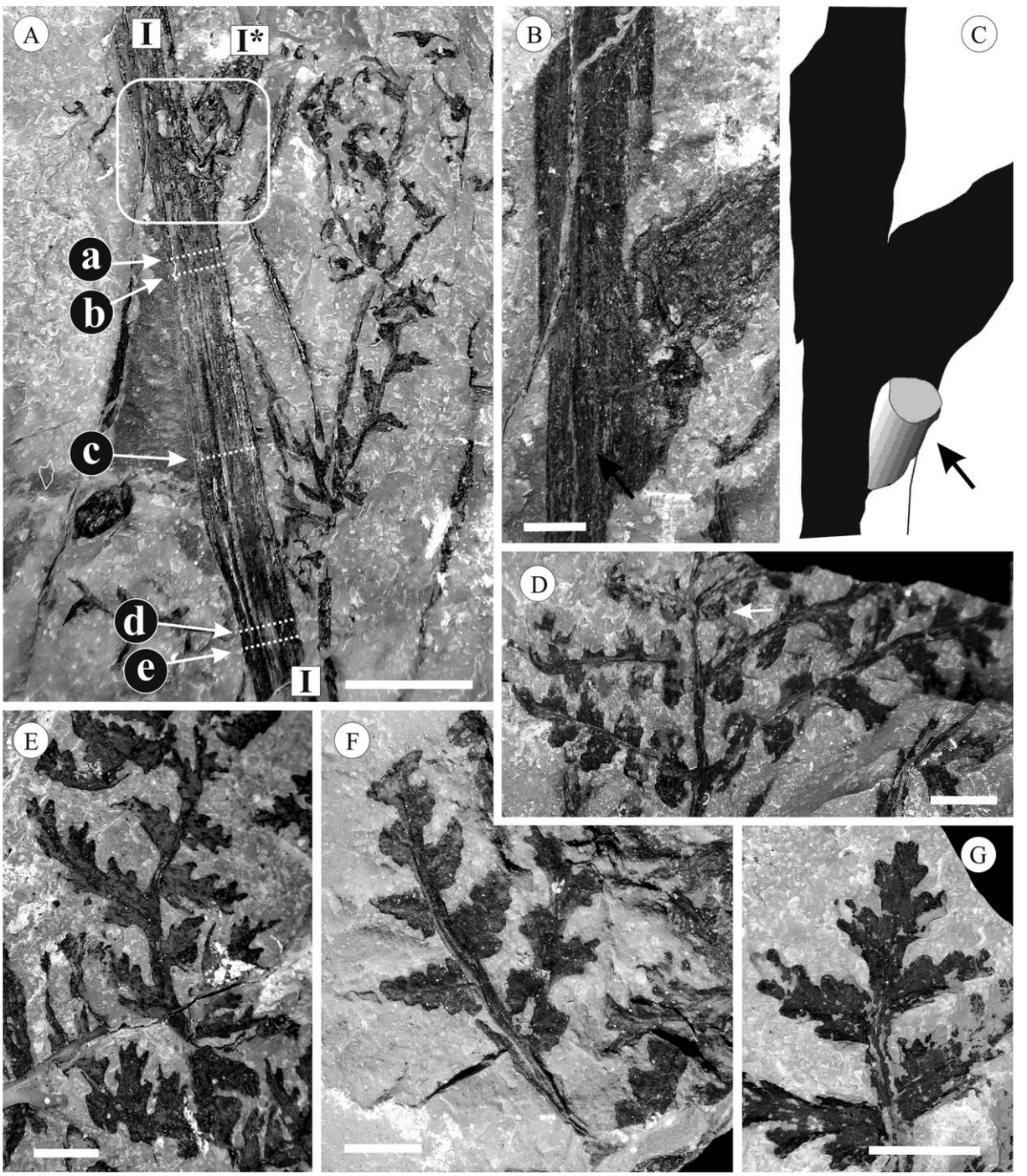

Fig. 6 *A*, Stem (I) with branch (I*) coming from node. Stem is associated with typical pinnules of this species. Labels a–e indicate positions of anatomical sections. Specimen PB23027. Scale bar = 10 mm. *B*, *C*, Detail of node, with outgoing branch and a short section of petiole (arrow) situated below the branch. Detail from frame in *A*. Scale bar = 2 mm. *D*, Distal part of middle-size frond/leaf bearing pinnules with developed pinnule laminae in the proximal part of the ultimate pinna and partly reduced pinnule laminae distally on the ultimate pinna. Specimen PB23031. Scale bar = 5 mm. *E*, Distal part of a large frond, showing distinctive asymmetry of significantly lobate pinnules. Specimen PB23028. Scale bar = 5 mm. *F*, Distal part of middle-size frond/leaf, showing distinctive asymmetry consisting of lobate pinnules terminated by pinnules with fully developed pinnule lamina. Specimen PB23029. Scale bar = 5 mm. *G*, Distal part of a large frond, showing significantly lobate pinnules terminated by a trilobate apical pinnule. Specimen PB23030. Scale bar = 5 mm. A color version of this figure is available online.

This content downloaded from 147.188.216.059 on July 06, 2020 04:23:42 AM
All use subject to University of Chicago Press Terms and Conditions (http://www.journals.uchicago.edu/t-and-c).

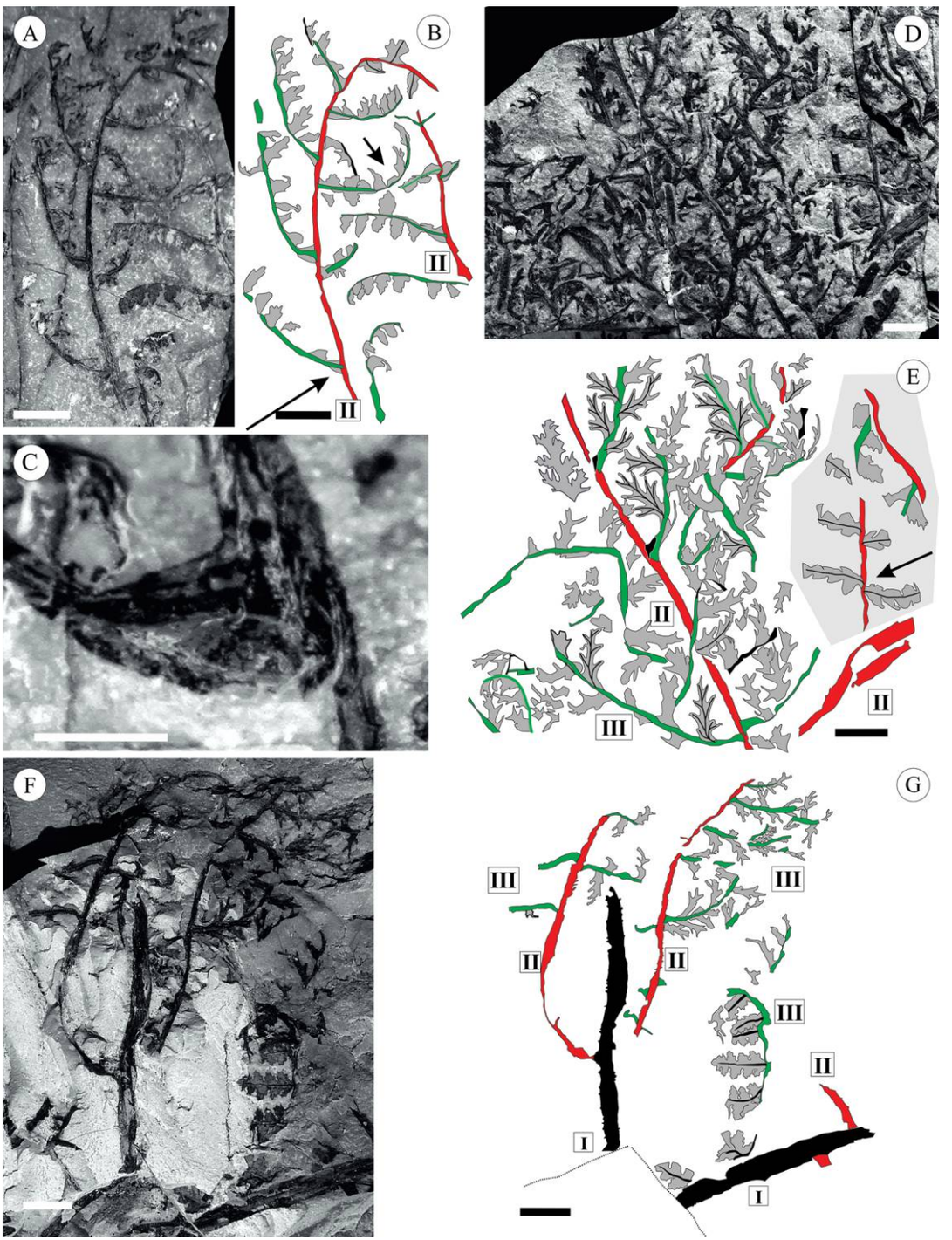

Fig. 7 *A*, Two middle-size fronds/leaves of *Wudaeophyton wangii* gen. et sp. nov. Specimen PB23026. Scale bar = 10 mm. *B*, Camera lucida drawing of specimen from *A*. Red rachises indicate frond/primary rachis; green rachises indicate ultimate rachises. II = frond/primary rachis. Scale bar = 10 mm. *C*, Outgoing point of an ultimate rachis from a frond rachis. Small triangular to tongue-shaped pinnule is attached to the frond rachis. Detail from *A*. Scale bar = 3 mm. *F*, Distal part of a large frond, showing distinctive asymmetry of significantly lobate pinnules. Specimen PB23028. Scale bar = 5 mm. *D*, Fragment of the middle part of a large frond/leaf with many lobate pinnules. Specimen PB23032. Scale bar = 10 mm. *E*, Camera lucida drawing of specimen from *D*. Red rachises indicate frond/primary rachis; green rachises indicate ultimate rachises. Arrow points to small fragment of small frond/leaf. II = frond/primary rachis; III = ultimate rachis. Scale bar = 10 mm. *F*, Stem and two fronds/leaves. Scale bar = 10 mm. *G*, Line drawing from photograph of the specimen lost during transport from locality. Black rachises indicate the stem, red rachises indicate the frond/primary rachis, and green rachises indicate the ultimate rachises. I = stem; II = frond/primary rachis; III = ultimate rachis. Scale bar = 10 mm.

This content downloaded from 147.188.216.059 on July 06, 2020 04:23:42 AM
All use subject to University of Chicago Press Terms and Conditions (http://www.journals.uchicago.edu/t-and-c).

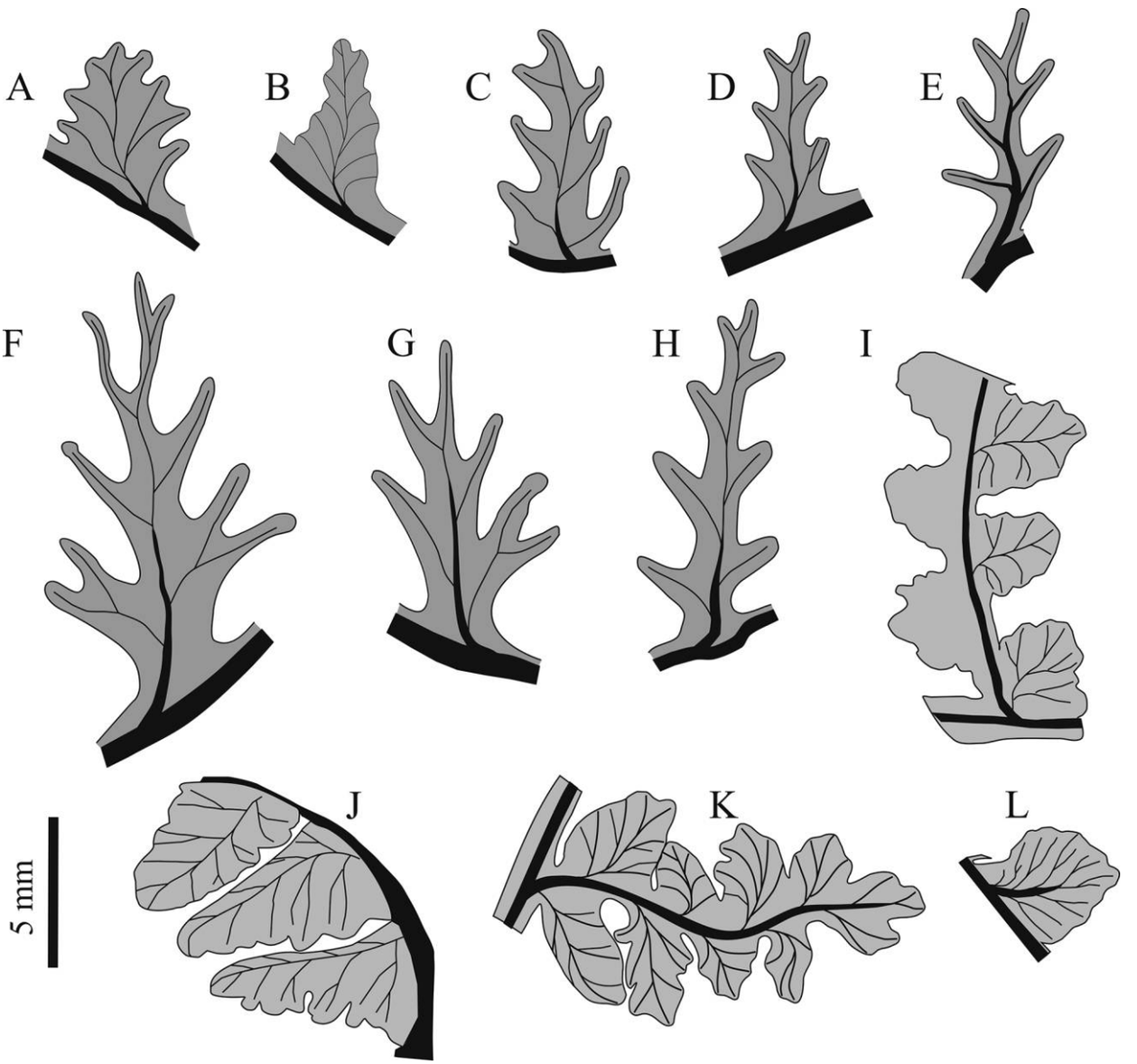

Fig. 8 Pinnule variability of *Wudaeophyton wangii* gen. et sp. nov. *A*, Basalmost basiscopic pinnule with many small lobes marginally, mostly placed in the distal parts of large- and middle-size fronds/leaves. *B*, Laminate pinnule with small lobes on margin, mostly placed in distal part of middle-size fronds/leaves. *C*, Pinnule with reduced lamina and well-developed lobes, mostly placed in distal part of large middle part of middle-size fronds/leaves. *D*, Pinnule with reduced lamina and partly developed lobes, distributed in both large- and middle-size fronds/leaves. *E*, Pinnule with reduced lamina and well-developed lobes that occurred in distal end of the ultimate pinnae of large- and middle-size fronds/leaves. *F*, Pinnule with reduced lamina and well-developed lobes from the middle part of the ultimate pinnae of large-size fronds/leaves. *G*, Pinnule with reduced lamina and well-developed lobes from the proximal part of the ultimate pinnae of large-size fronds/leaves. *H*, Pinnule with reduced lamina and well-developed lobes that occurred in the middle part of the ultimate pinnae of the lower part of large-size fronds/leaves. *I*, Laminate pinnule with small marginal lobes, mostly in the distal part of middle-size fronds/leaves. *J*, Laminate linguae-shaped pinnule with entire or "imperceptible" small marginal lobes, occurring in the proximal part of large fronds/leaves. Similar forms occurred in small fronds/leaves. *K*, Laminate pinnule with entire or "imperceptible" small marginal lobes, positioned in the proximal part of large- and middle-size fronds/leaves. *L*, Delta-form laminate pinnules from the middle part of small fronds/leaves.

the right side (short arrow in fig. 7*B*). Specimen PB23031 (fig. 6*D*) shows the upper and middle parts of this pinna type where several ultimate pinnae arise oppositely and subopposite from the frond (primary) rachis. Pinnules on the ultimate pinna have well-developed pinnule laminae on the proximal parts of the ultimate pinna and partly reduced laminae distally (fig. 6*D*). The presence of different types of pinnule on a single ultimate unit is typical of fronds of this species. Distal parts of medium-size fronds/leaves also show distinctive asymmetry and consist of lobate pinnules (fig. 6*F*) terminated by pinnules with fully

This content downloaded from 147.188.216.059 on July 06, 2020 04:23:42 AM
All use subject to University of Chicago Press Terms and Conditions (http://www.journals.uchicago.edu/t-and-c).

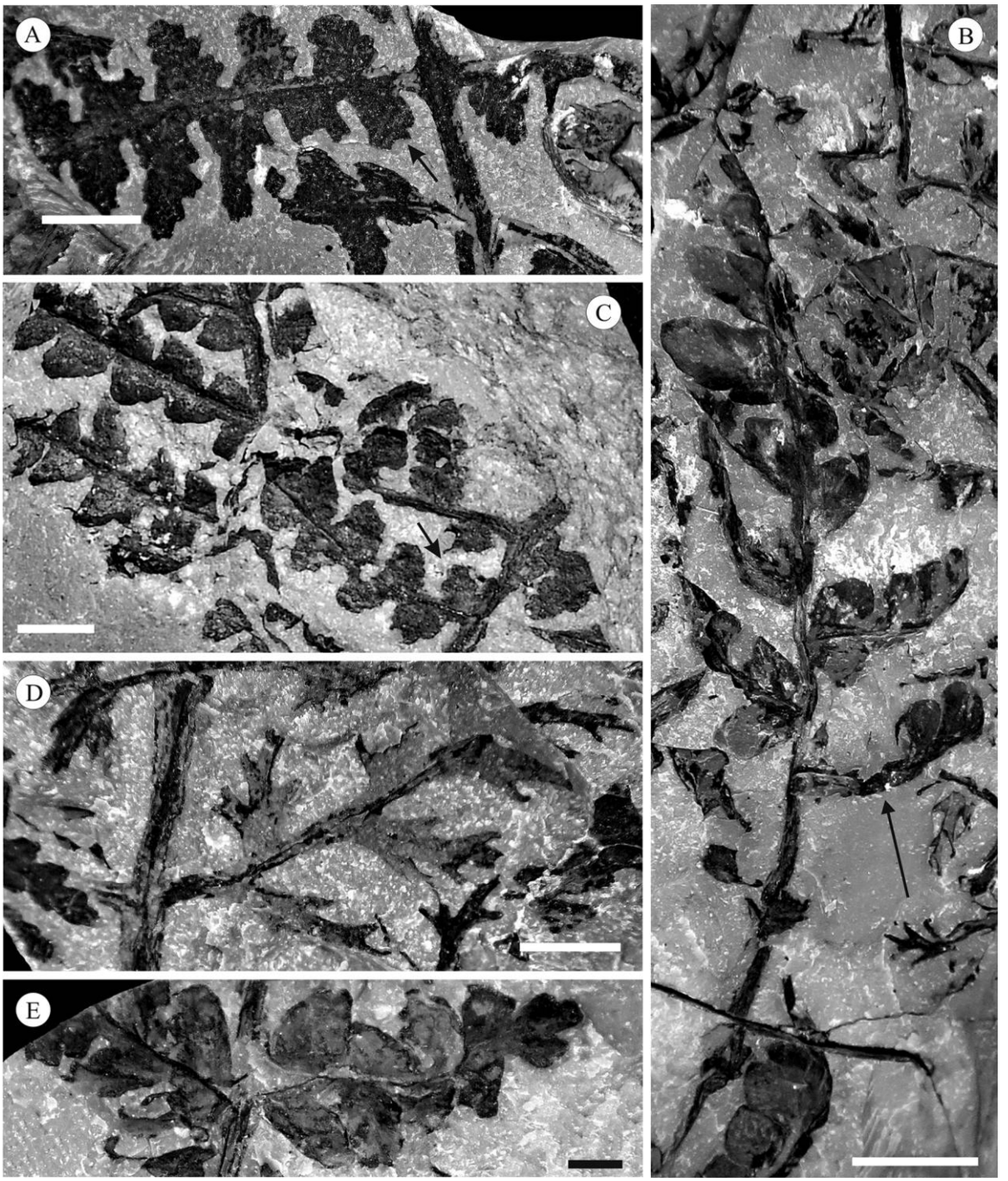

Fig. 9 Ultimate pinnae variability of *Wudaeophyton wangii* gen. et sp. nov. *A*, Ultimate pinna bearing pinnule with fully developed pinnule lamina. Pinnules are asymmetric, with more distinctly lobed side toward frond rachis, and proximal pinnules are smaller than those on the middle part of ultimate pinnae. Lowermost basiscopic pinnule is situated close to frond rachis (arrow). Specimen PB23035. Scale bar = 5 mm. *B*, Pinnule with developed pinnule lamina and small blunt lobes from small frond/leaf. Arrow shows position of tongue-shaped pinnules. Specimen PB23038. Scale bar = 10 mm. *C*, Specimen showing several ultimate pinnae attached to the frond rachis. Pinnules are laminate, triangular in shape, with "imperceptible" lobes or nearly entire margin. Arrow points to lowermost basiscopic pinnule attached to both the frond rachis and the ultimate rachis with preserved intercalary features. Specimen PB23037. Scale bar = 5 mm. *D*, Lower part of ultimate pinna from large fronds/leaves bearing deeply lobate pinnules. Specimen PB23039. Scale bar = 5 mm. *E*, Two short ultimate pinnae attached to frond rachis close to point attached to stem. Pinnae bear small tongue-shaped pinnules with fully developed pinnule laminae. Specimen PB23040. Scale bar = 2 mm.

This content downloaded from 147.188.216.059 on July 06, 2020 04:23:42 AM
All use subject to University of Chicago Press Terms and Conditions (http://www.journals.uchicago.edu/t-and-c).

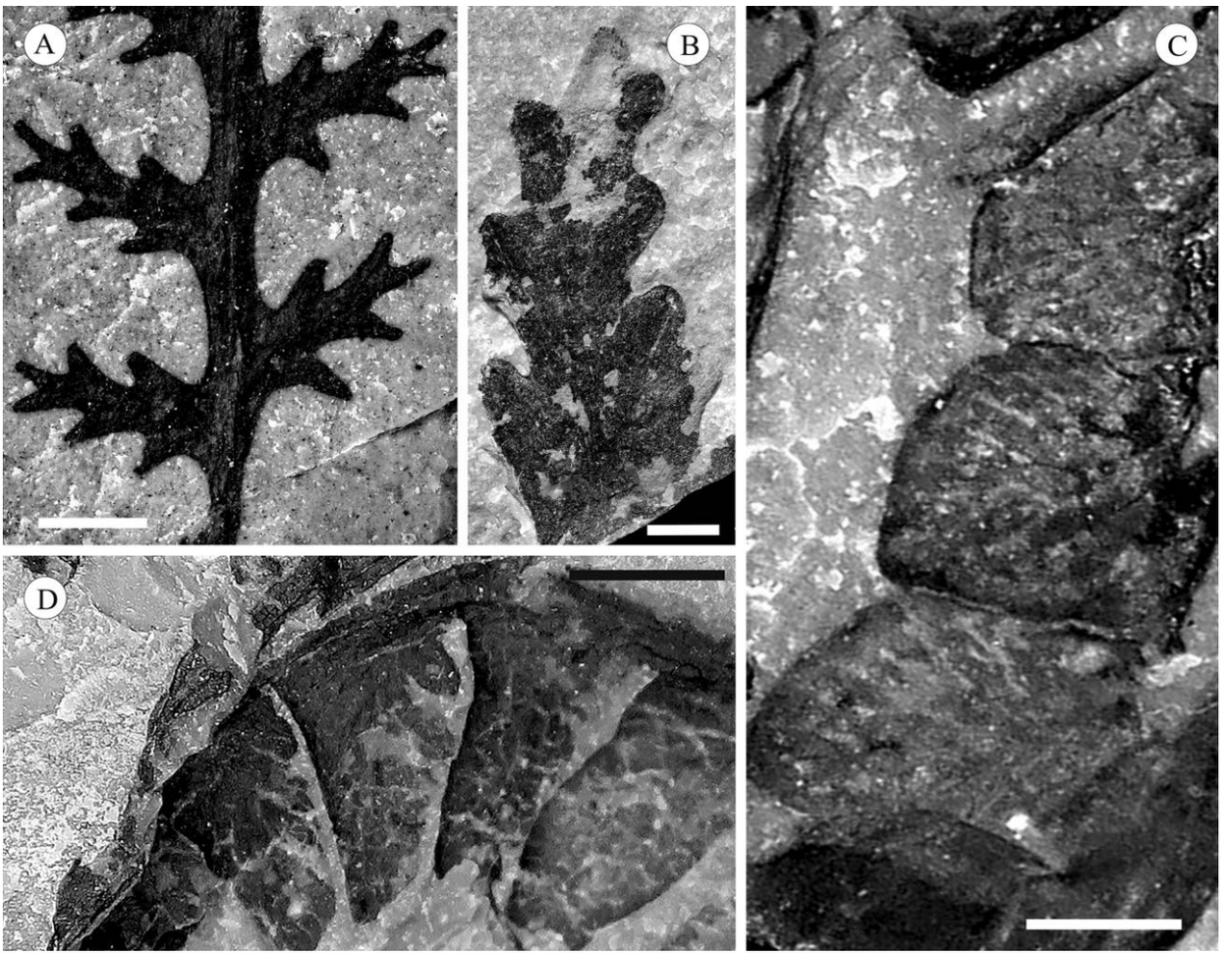

Fig. 10 Major types of pinnules of *Wudaeophyton wangii* gen. et sp. nov. *A*, Typical deeply lobate pinnules with pinnule climbing adaptations. Specimen PB23041. Scale bar = 3 mm. *B*, Transition form between deeply lobate and lobate forms, where lobes are not developed into linear structures from distal part of large fronds/leaves. Specimen PB23030. Scale bar = 1 mm. *C*, Delta-form pinnules from approximately halfway (middle and distal) along a small frond/leaf. Specimen PB23036. Scale bar = 2 mm. *D*, Ultimate pinna with tongue-shaped pinnules and fully developed pinnule laminae and "imperceptible" small lobes on the side toward the frond rachis from the small frond/leaf. Specimen PB23036. Scale bar = 3 mm.

developed pinnule laminae. Tips of large- and medium-size fronds consist of trilobate pinnules (fig. 6*G*) that may in some cases be elongated.

The smallest fronds are ca. 50–100 mm long and bear only tongue-shaped pinnules with fully developed pinnule laminae (fig. 9*B*). They are often situated in the proximal parts of branched stems (figs. 4*B*, 5*C*, II).

The frond rachis (primary rachis) is straight (fig. 4*A*, 4*B*) and is typically 1.5–2 mm wide. Rachises bear eccentrically organized short prickles similar to those on the stem. These are 180–200 μm long and 200–300 μm wide. Prickles on the frond rachis have drop-shaped bases (fig. 5*F*). Ultimate pinnae are opposite (figs. 6*D*, 9*A*, 9*C*, 9*D*) or subopposite (figs. 7*A*, 7*B*, 9*B*); are slightly asymmetric, with basiscopic pinnules being slightly smaller than acroscopic pinnules; and are perpendicularly inserted onto the frond rachis. In the lower and middle parts of the frond, ultimate pinnae are oppositely organized, while toward the tip of the ultimate pinna, they are subopposite and alternate proximally (fig. 7*A*, 7*B*). The departure point of the ultimate rachis from the frond rachis is accompanied by a small triangular to tongue-shaped pinnule (fig. 7*C*) that is attached to the frond (primary) rachis. This kind of pinnule is present on all specimens where attachment of the ultimate rachis to the frond rachis is preserved. It is unclear whether this kind of pinnule was free or whether it developed together with the ultimate rachis. Ultimate pinnae vary in size from 12 to 60 mm long and are asymmetric with a lanceolate outline (figs. 6*D*, 9*A*). The ultimate rachis is straight and is 0.4–1.2 mm wide.

Pinnules

Significantly heterophyllous pinnules alternate on the ultimate rachis (fig. 8); these can be distinguished into several forms. Generally, the venation is poorly visible on nearly all of the specimens. Together with the fact that the coal film preserving the pinnules is thick, it appears that the pinnules were thick and pulpous. All of the pinnule types of this species have identical

This content downloaded from 147.188.216.059 on July 06, 2020 04:23:42 AM
All use subject to University of Chicago Press Terms and Conditions (http://www.journals.uchicago.edu/t-and-c).

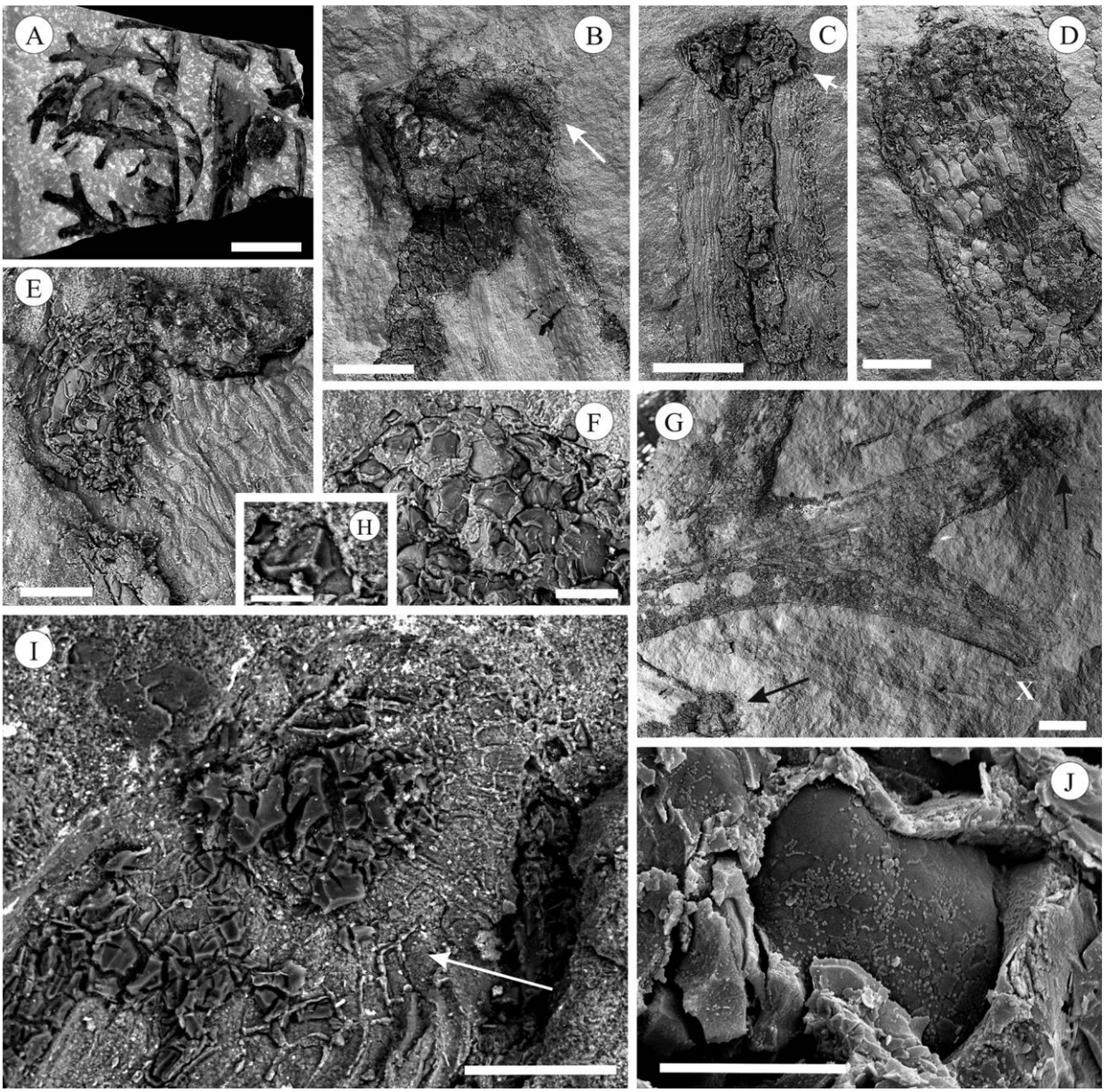

Fig. 11 Climbing structures of *Wudaeophyton wangii* gen. et sp. nov. from specimen PB23043—counterpart of the holotype PB23025 slab. Image *A* under macrophotography, *B–J* under SEM. *A*, Specimen showing deeply lobate pinnules with pinnule climbing adaptations. Scale bar = 5 mm. *B*, Detail of globose pad situated in the tip of a pinnule lobe tendril with distinct annular structure (arrow). Scale bar = 250 μm. *C*, Pads connected to vestigial vascular system. Only lowermost pad is preserved. Arrow points to a row of slightly different elongate cells situated between pad and the top of the tendril. Scale bar = 250 μm. *D*, Details of a tendril with partially recognizable "neck" between the tendril and pad. Scale bar = 250 μm. *E*, Pair of buds in the tip tendril. Scale bar = 100 μm. *F*, Polygonal cells on the pad. Scale bar = 50 μm. *G*, Details of two pinnule climbing adaptations. Two arrows point to globose pads, while X shows the end of a tendril where the pad is missing. Scale bar = 0.5 mm. *H*, Trilete, laevigate small dispersed miospore of the *Leiotriletes* type adhered to the surface of these pad cells. Scale bar = 25 μm. *I*, Apical part of tendril with remains of pad. Arrow points to a row of slightly different elongate cells situated between pad and the top of the tendril. Scale bar = 100 μm. *J*, "Resin body" in pad cells. Scale bar = 10 μm.

epidermal structures (see below), and in many cases two or more pinnule types are attached to the same rachis (fig. 6*D*). All pinnules are narrowly linguaeform or triangular in outline, with their entire bases inserted into the ultimate rachis. Individual pinnules are slightly or entirely asymmetrical (e.g., fig. 10*A*), with lobed margins consistently oriented, to varying degrees, toward the frond (primary) rachis. Generally, venation is difficult to discern in pinnules with fully developed pinnule laminae from which veins appear to be embedded in the thick mass of the lamina. The midvein is nearly straight and thick and is wider proximally than

This content downloaded from 147.188.216.059 on July 06, 2020 04:23:42 AM
All use subject to University of Chicago Press Terms and Conditions (http://www.journals.uchicago.edu/t-and-c).

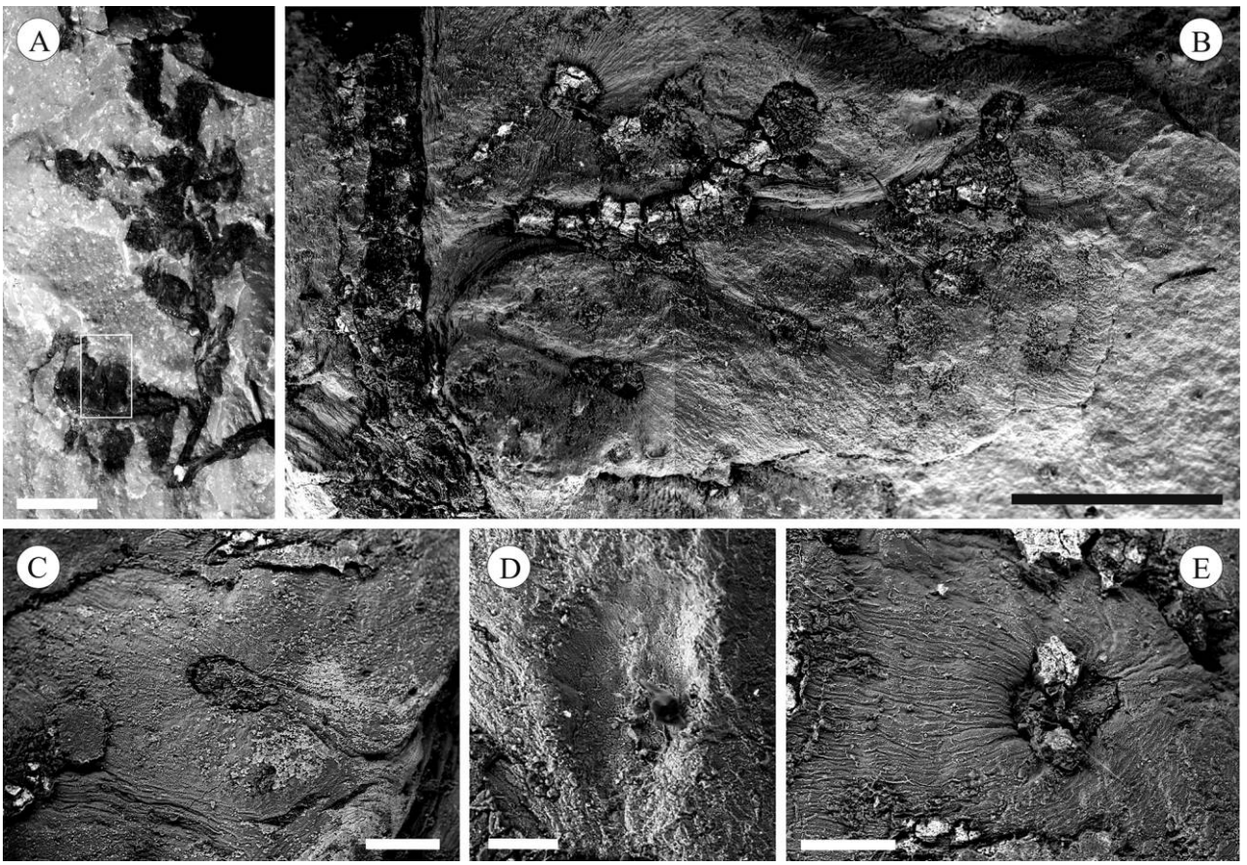

Fig. 12 Possible fertile pinnules of *Wudaeophyton wangii* gen. et sp. nov. from specimen PB23044. *A*, Fertile pinnules with fully developed pinnule lamina. Scale bar = 5 mm. *B*, Details from SEM of a fertile pinnule bearing imprints of missing, probably reproductive, organs, preserved as coal in the center of a rounded structure. Scale bar = 1 mm. *C*, Vascular system with lateral veins ending in the center of a rounded structure. Scale bar = 50 μm. *D*, SEM image showing some features of the attachment point, sometimes represented by a "hole." Scale bar = 100 μm. *E*, SEM image showing centrifugal, striated, rounded structures occupying almost the entire pinnule surface on the whole side of the midvein, with coal-filled field areas in the centers. Scale bar = 200 μm.

distally. Lateral veins are simple (fig. 8*B*–8*E*, 8*H*) or divide once (fig. 8*A*, 8*F*, 8*G*, 8*I*, 8*K*–8*L*) or occasionally twice (fig. 8*J*) in pinnules with fully developed pinnule laminae. The vein density is usually five to seven veins per centimeter of pinnule margin in pinnules with well-developed pinnule laminae, and there is around one vein in pinnules with well-developed lobes.

Pinnules with well-developed long, linear lobes and reduced pinnule laminae (figs. 9*D*, 10*A*, 11*A*) conform to the *Rhodeopteridium* type, dominate the fossil record at the Wuda locality (fig. 8*E*–8*H*), and belong to this plant species. They occur mainly in large fronds/leaves (fig. 7*D*–7*G*) but also in medium-size fronds/leaves (fig. 6*D*). Individual pinnules are 5–13 mm long and 4–5 mm wide (fig. 9*A*) and vary from five to nine (typically six) lobes per pinnule. This large number of pinnule lobes (fig. 8*F*) is typical for large pinnules that occur in large fronds/leaves (fig. 7*D*). They often have dichotomized lateral veins in their proximal parts (fig. 8*F*, 8*G*). Lobes are linear, with distinctive slightly swollen tips and well-developed pads; we term these pinnule climbing adaptations (see below). Figure 11*A* shows reduction of a pinnule lamina in large pinnules where the lamina is well preserved only in the axil of the midvein and lateral veins.

Pinnules with partly reduced laminae and shorter lobes belong to the second common pinnule form (fig. 8*C*, 8*D*). These pinnules are 4–8 mm long, 3–4 mm wide, and lobate (fig. 8*C*). The number of lobes varies from five to seven per pinnule, and lobes are short and linear with a distinct tip. The pinnule in figure 10*B* represents a transitional form between the deeply lobate forms and lobate forms; the pinnule is 7 mm long, but lobes do not develop into linear structures.

Another common pinnule type is represented by pinnules with a weakly developed pinnule lamina. Lobes vary between forms that are bluntly lobed, that have small lobes (fig. 9*A*), and that have weakly lobed margins (figs. 8*B*, 8*I*, 9*A*). Their affiliation to pinnules bearing pinnule climbing adaptations is demonstrated in specimen PB23031 (fig. 6*D*), where both types are preserved in a single ultimate pinna. These pinnules are 3–6 mm long and 2–3 mm wide.

The most common pinnule morphology is represented by small deltoid or triangular-shaped laminate pinnules with well-developed lobes or with weakly lobed or entire margins (figs. 9*C*, 10*C*). Pinnules of this kind conform to the *Pseudomariopteris-Emplectopteris* type and mainly occur in small fronds (figs. 8*L*,

This content downloaded from 147.188.216.059 on July 06, 2020 04:23:42 AM
All use subject to University of Chicago Press Terms and Conditions (http://www.journals.uchicago.edu/t-and-c).

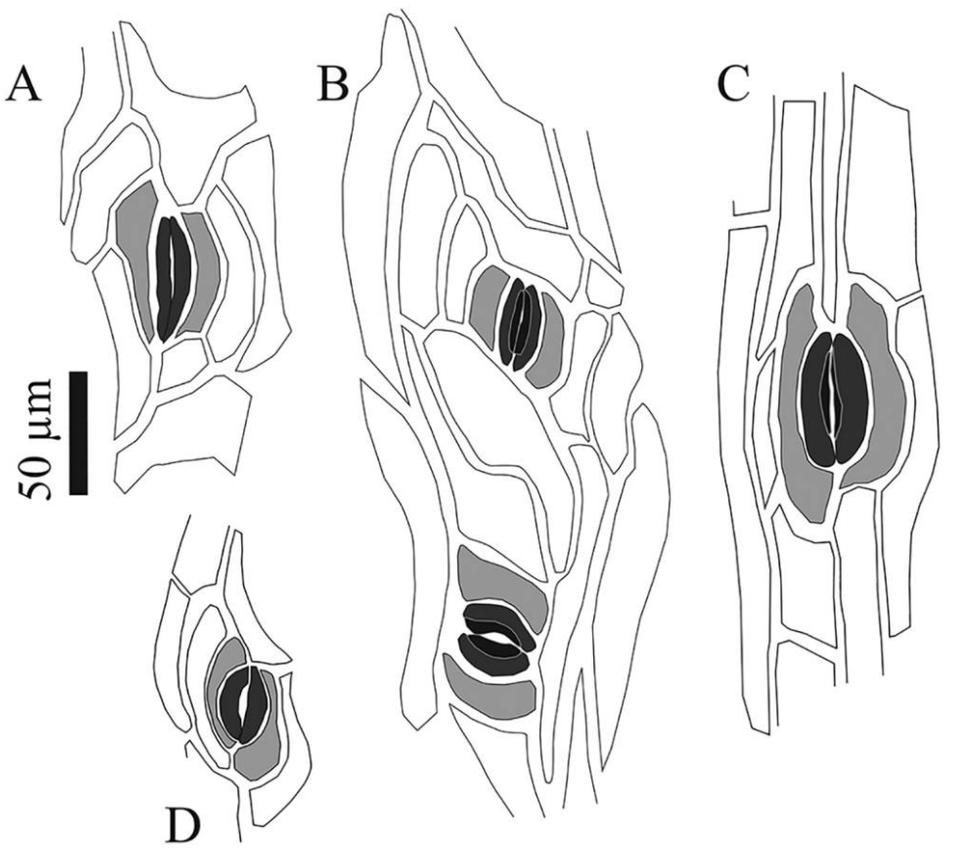

Fig. 13 Paracytic stomatal apparatus from pinnules and rachis of *Wudaeophyton wangii* gen. et sp. nov. *A*, Stomatal apparatus from vegetative pinnules with reduced pinnule laminae. *B*, Stomatal apparatuses from vegetative pinnules with partly reduced lamina. *C*, Stomatal apparatus from the frond rachis. *D*, Stomatal apparatus from fertile pinnules.

9*B*). Individual pinnules of this type are 2–3 mm long and ca. 3 mm wide (arrow in fig. 7*E*).

An additional pinnule form associated with large pinnules is represented by tongue- or deltoid-shaped pinnules (figs. 8*J*, 8*K*, 9*E*, 10*D*), which are again associated with this species because of their epidermal structures (see below). Pinnules are 3–5 mm long and ca. 3 mm wide, with margins appearing to be straight or having generally imperceptible small lobes. They also occur in the holotype slab, but in that specimen their exact position on the frond/leaf is undeterminable. Another area with this type of pinnule is situated in the middle part of the holotype. In this specimen, pinnules are attached to short ultimate rachises and are inserted onto the primary rachis of small fronds, which is outgoing from the proximal part of the branched stem (fig. 5*C*). These pinnules are also preserved in specimen PB23036 in the middle parts of a small frond/leaf (arrow in fig. 9*B*). According to these examples from the holotype slab and specimen PB23036, this type of pinnule occurs in both the proximal parts of large, medium, and small fronds. Another slightly different type of pinnule occurs in the basalmost position of the basiscopic side of the ultimate pinnae. These basalmost pinnules are generally smaller and wider with different degrees of lobe development (fig. 8*A*). The lowermost basiscopic pinnules vary from having straight margins (fig. 9*C*, arrow) to being slightly lobate (arrow in fig. 9*A*) to being lobate or significantly lobate, creating linear lobed structures (fig. 8*A*). These pinnules can have intercalary characters (arrow in fig. 9*C*).

Pinnule Climbing Adaptations

Most large pinnules have linear lobes terminated by swollen structures (fig. 11*A*) that are recognized as adhesive pads. Linear lobes (fig. 11*G*) are 1.5–2.2 mm long and 0.5 mm wide and originally were probably cylindrical conical.

In many cases there is a partially visible neck between the pads and the linear lobes of the pinnule climbing adaptations (fig. 11*I*), but less often their transition is almost imperceptible (fig. 11*D*). Terminal pads are vascularized (fig. 11*C*), although poor preservation prevents this from being further characterized. The area between the pad and the linear lobe consists of elongated cells 30–50 μm long and 10–20 μm wide (arrows in fig. 11*C*, 11*I*). Mostly, lobes are terminated by only one pad, but occasionally two pads are situated at the tip of a lobe (figs. 9*E*, 11). In some instances, pinnule lobes appear to be losing their pads (X in fig. 11*G*), and only proximal parts are preserved (fig. 11*C*). Pads are globose (figs. 9*B*, 11) and ca. 500 μm in diameter. There is a distinct annular structure present at the distal margin of individual pads (arrow, fig. 11*B*), with this being ca. 250 μm in diameter and comprising a band of cells that is ca. 100 μm wide. The band consists of two or three rows of

This content downloaded from 147.188.216.059 on July 06, 2020 04:23:42 AM
All use subject to University of Chicago Press Terms and Conditions (http://www.journals.uchicago.edu/t-and-c).

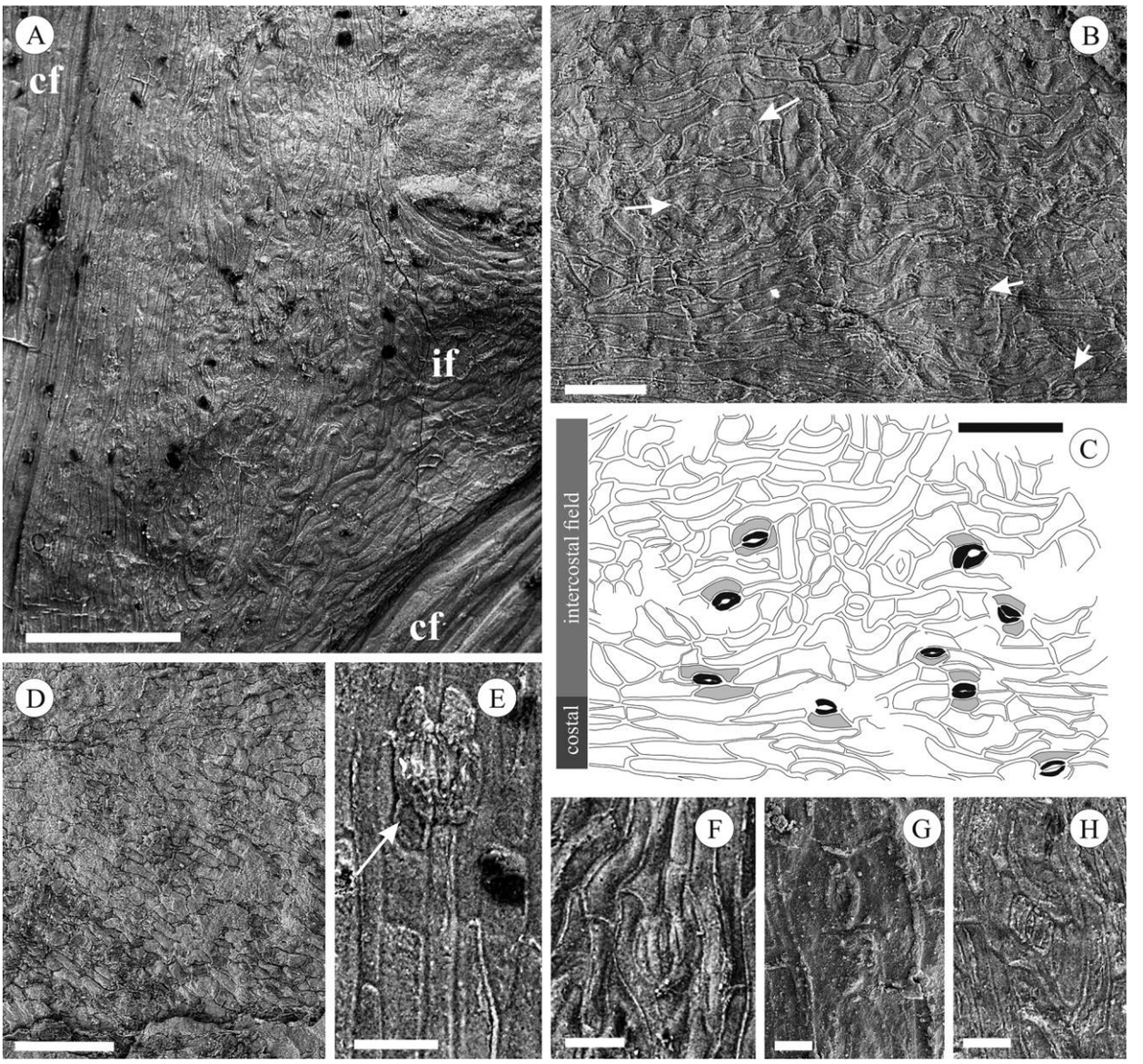

Fig. 14 SEM images of epidermal structures of *Wudaeophyton wangii* gen. et sp. nov. from the holotype PB23025. *A*, Epidermal structures of lower side of deeply lobate pinnules. Lamina is reduced into the axil and a narrow strip area alongside the veins. Epidermal structures are different in costal fields (cf) and intercostal fields (if). Scale bar = 250 μm. *B*, Features from the lower side of a pinnule, mostly from the intercostal field, with irregularly distributed stomatal apparatuses. Scale bar = 100 μm. *C*, Redrawing of *B*. Gray fields represent subsidiary cells. Scale bar = 150 μm. *D*, Epidermal structure from the upper pinnule surface with represented polygonal elongated cells. Scale bar = 250 μm. *E*, Paracytic stoma with two distinct subsidiary cells from rachis. Scale bar = 50 μm. *F*, Paracytic stoma from the intercostal field of the lower pinnule surface. Scale bar = 50 μm. *G*, Paracytic stoma with two distinct subsidiary cells from the intercostal field of the lower pinnule surface. Scale bar = 20 μm. *H*, Paracytic stoma from the intercostal field of the lower pinnule surface. Scale bar = 50 μm.

small cells from 30 to 50 μm long and 20 to 30 μm wide that are slightly elongated and concentrically oriented (fig. 11*B*). Cell size is not uniform between pads and linear lobes. Cells of the linear lobes are tetragonal polygonal, 60–210 μm long, and 20–25 μm wide and are elongated parallel to the axis of the pinnule lobe. By contrast, cells of the pads are polygonal and ca. 50 μm in diameter (figs. 9*F*, 11). These cells situated in pads probably present secretory cells for adhesive fluid, with remains probably presenting just adhesive fluid (fig. 11*J*). The adhesive fluid nature is supported by the fact that different spores occur adhered to the surface (fig. 11*H*). These lobes are named pinnule climbing adaptations, with the name derived from their presumed function.

Possible Fertile Pinnules

Possible fertile pinnules are present in only one specimen (PB23044) but are incompletely preserved (fig. 12*A*). They are

This content downloaded from 147.188.216.059 on July 06, 2020 04:23:42 AM
All use subject to University of Chicago Press Terms and Conditions (http://www.journals.uchicago.edu/t-and-c).

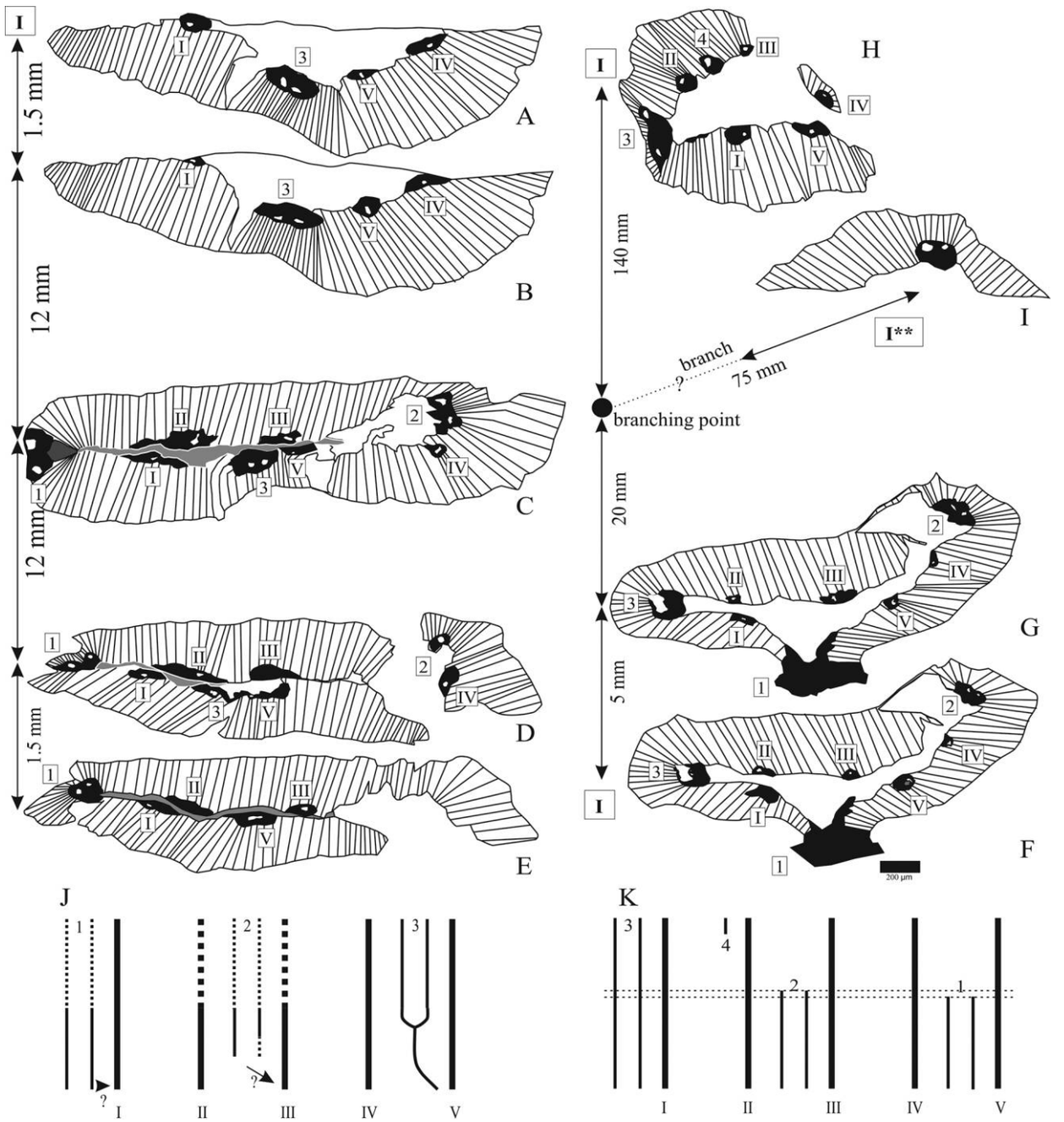

Fig. 15 Primary vascular system of the stem of *Wudaeophyton wangii* gen. et sp. nov. Black fields represent primary vascular bundle, with white-filled protoxylem strands inside; gray field inside represents parenchymatous pith; and hatch-marked area represents secondary xylem. Intervals on left side of each section show distances of anatomical section made from the stem. Roman numbers represent primary axial bundles, while numbers 1–3 represent leaf traces. I in rectangle = stem; I** in rectangle = branch/stem. *A–E*, Primary vascular structure of stem from specimen PB23027. *F–H*, Primary vascular structure of stem from holotype PB23025. *I*, Primary vascular structure of branch from holotype PB23025. *J*, Diagram of axial vascular system from specimen PB23027, where thick lines represent primary axial strands (roman numbers), thin lines represent leaf traces (numbered 1–3), and dashed lines represent predictable continuance of axial strands. *K*, Diagram of the axial vascular system from the holotype PB23025 with two nodes (dashed lines).

This content downloaded from 147.188.216.059 on July 06, 2020 04:23:42 AM
All use subject to University of Chicago Press Terms and Conditions (http://www.journals.uchicago.edu/t-and-c).

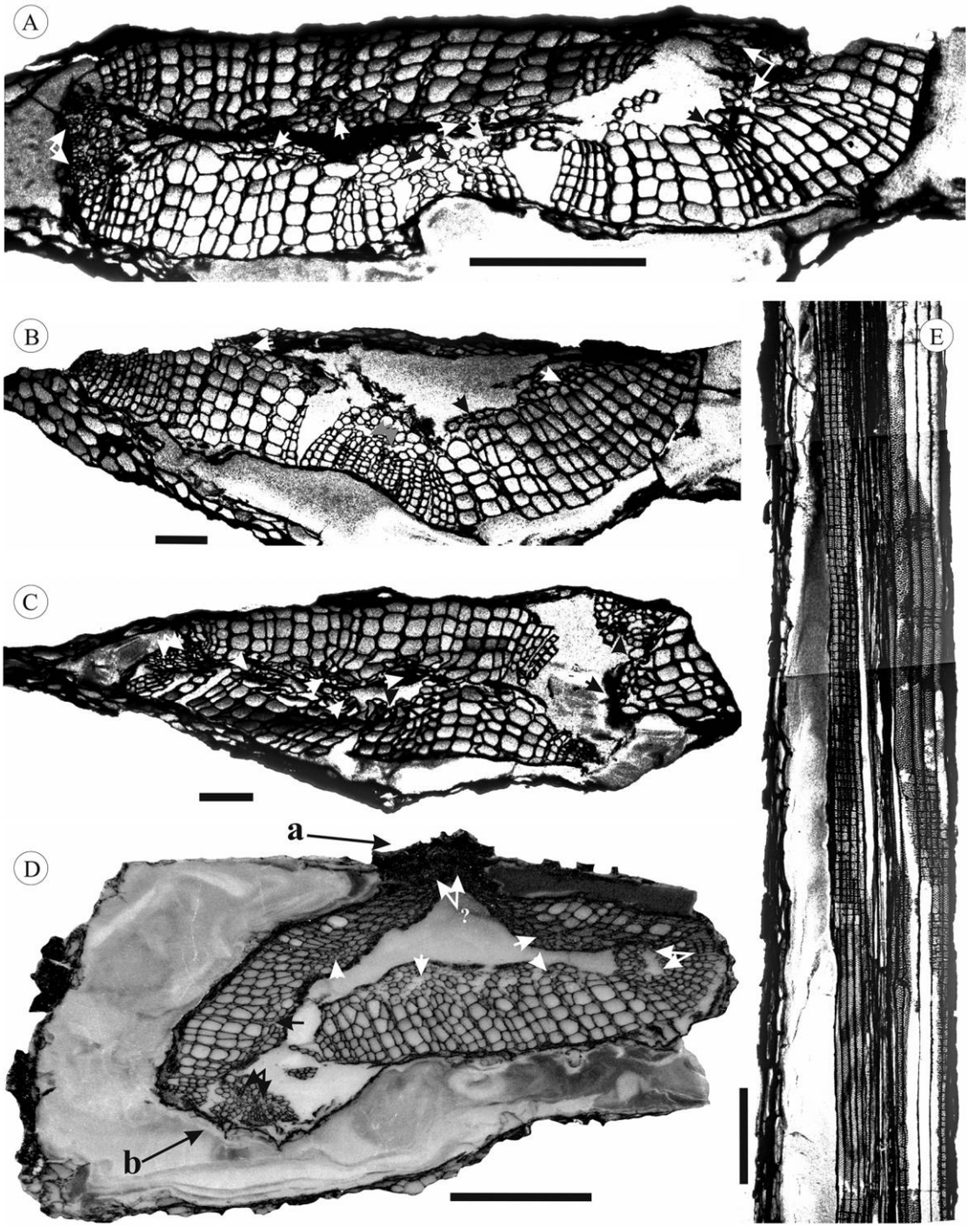

Fig. 16 Transverse and longitudinal sections of stems of *Wudaeophyton wangii* gen. et sp. nov. from specimen PB23027 (*A–C*) and holotype PB23025 (*D*). *A*, Nearly complete transverse section, with dark zone in pith containing remains of parenchyma cells, primary xylem bundles (arrows), leaf traces (double arrows), secondary xylem, and occasionally preserved cells of the outer cortex. Section c from figure 6*A*. Scale bar = 0.5 mm. *B*, Tangentially split stem showing primary xylem bundles (arrows), leaf traces (double arrows), secondary xylem, and occasionally preserved cells of the outer cortex, including cells with amber-colored contents. Section a from figure 6*A*. Scale bar = 0.2 mm. *C*, Nearly complete transverse section showing primary xylem bundles (arrows), leaf traces (double arrows), secondary xylem, and occasionally preserved cells of the outer cortex. Section d from figure 6*A*. Scale bar = 0.2 mm. *D*, Nearly complete transverse section showing pith (lacking cell structures), primary xylem bundles (arrows), leaf traces (double arrows), secondary xylem, and occasionally preserved cells of outer cortex. Label a indicates leaf trace with estimated bud (no recognizable cell structures); b indicates leaf trace entering into petiole in subsequent node. Section g from figure 4*A*. Scale bar = 0.5 mm. *E*, Longitudinal section showing primary xylem in center followed by secondary xylem with visible rays. Cell structure between secondary xylem and outer cortex is missing, and outer cortex cells are partly preserved. Scale bar = 0.5 mm.

This content downloaded from 147.188.216.059 on July 06, 2020 04:23:42 AM
All use subject to University of Chicago Press Terms and Conditions (http://www.journals.uchicago.edu/t-and-c).

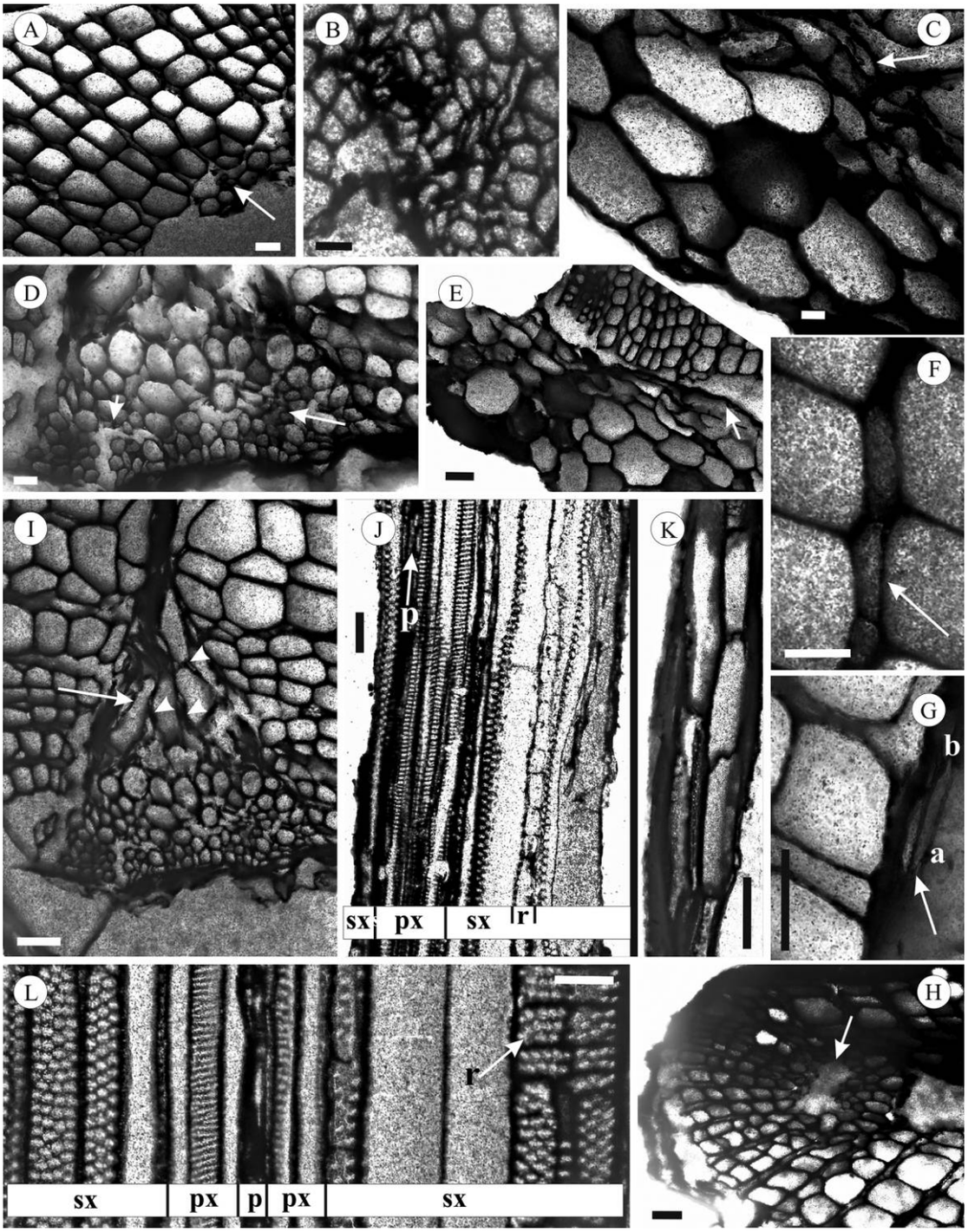

Fig. 17 Detailed anatomical structures from stems of *Wudaeophyton wangii* gen. et sp. nov. *A*, Detail of the primary xylem situated inside the secondary xylem. Arrow points to small tracheids, probably protoxylem, surrounded by metaxylem tracheids. Specimen PB23027. Scale bar = 50 μm. *B*, Detail of a double-stranded leaf trace. Primary xylem bundles show dark center surrounded by protoxylem and metaxylem tracheids with mesarch development. Specimen PB23027. Scale bar = 20 μm. *C*, Large cells of the outer cortex with dark amber-colored cell contents. Smaller tangentially elongated cells situated on the inner side of the preserved cortex zone (arrow). Specimen PB23027. Scale bar = 20 μm. *D*, Enlargement of a double-stranded leaf trace. Primary xylem bundles (arrows) show small area surrounded by protoxylem and metaxylem tracheids with mesarch maturation. Specimen PB23027. Scale bar = 50 μm. *E*, Large cells of the outer cortex with dark amber-colored cell contents; thin dark zone at arrow probably represents periderm. Specimen PB23027. Scale bar = 50 μm. *F*, Transverse view of uniserial ray cells (arrow) between secondary xylem cells. Specimen PB23027. Scale bar = 20 μm. *G*, Cells appearing to represent the vascular cambium (arrow), with fusiform initials represented by tangentially elongated cell (a), while ray initial is represented by tangentially shorter cells (b) in transverse section. Specimen PB23027. Scale bar = 50 μm. *H*, Detail of a double-stranded leaf trace. Primary xylem strand shows cell lacking cores (arrow), which are gathered together and surrounded by protoxylem and metaxylem tracheids, which are more developed on the inside of the primary xylem bundles. Holotype

This content downloaded from 147.188.216.059 on July 06, 2020 04:23:42 AM
All use subject to University of Chicago Press Terms and Conditions (http://www.journals.uchicago.edu/t-and-c).

similar to the vegetative pinnules with well-developed pinnular laminae in overall structure, and they have the same lobate character and identical epidermal structures, including the type of stomata (fig. 13*D*). These pinnules are 3.5–4.5 mm long and ca. 2.5 mm wide; are tongue shaped or triangular; are lobed, with each lobe blunt; and have fully developed laminae (fig. 12*A*). Venation is simple, with undivided lateral veins. On the abaxial (lower) pinnule surface, between the middle of the pinnule margin and the midvein (fig. 12*B*), there is an impression that is embedded into the pinnule lamina and that forms a hole (fig. 12*D*) or a coalified mound of tissue (fig. 12*C*, 12*E*) in the center of the impression. Fertile organs themselves are not present. The impression structure is rounded; is ca. 1 mm in diameter; and is centrifugally striated, occupying almost the entire pinnule surface to the side of the midvein. The hole or mound of tissue in the center of the impression represents the position and vestigial tissues of the vascular bundle that supplied the reproductive organs (fig. 12*C*).

Epidermal Structure

Epidermal structures are preserved as impressions in the fine-grained ash containing the fossils and are observed under SEM. It is possible to determine whether the imprints are of the lower or upper pinnule surfaces only in cases where individual pinnules are preserved in 3D with both sides present in the ash.

Epidermal cells on the frond (primary) rachis are more or less tetragonal, elongated, 50–150 μm long, and 15–30 μm wide (figs. 5*F*, 14*E*). Anticlinal walls are straight. Stomatal apparatuses occur on the frond rachises (fig. 14*E*) and consist of two distinct subsidiary cells and two guard cells forming the stomata (fig. 13*C*). Stomata are 50–70 μm long and 30–50 μm wide, with guard cells 11 μm wide. The long axis direction of the stomata corresponds with the position of the rachis axis. From epidermal cells on the frond, stomatal density (SD) is nine per 1 mm^2, and the stomatal index (SI) is 1.7.

Epidermal cells on the pinnules vary between the costal and intercostal fields (fig. 14*A*). Cells on the adaxial (upper) pinnule surface from costal fields are tetragonal polygonal, elongated, 100–140 μm long, and 10–18 μm wide. In contrast, those of the intercostal field are similar but are shorter and wider, 80–109 μm long, and 18–42 μm wide (fig. 14*D*) and are more or less oriented with their long axis parallel to the pinnule veins. Anticlinal walls are straight. Trichomes and stomatal apparatuses are absent on the pinnule epidermis.

On the abaxial (lower) pinnule surface, costal epidermal cells are tetragonal polygonal, elongated, 180–250 μm long, and 12–23 μm wide, while intercostal cells are irregular, polygonal, 30–150 μm long, and 18–40 μm wide (fig. 14*B*, 14*C*). Anticlinal walls are straight. Stomatal apparatuses are irregularly scattered on the abaxial surface and are distributed mainly in intercostal fields and sparsely in costal fields (fig. 14*B*, 14*C*). Stomatal apparatuses are paracytic, consisting of two guard cells and two subsidiary cells, with these situated on either side of the stoma, parallel to the long axis of the guard cells (figs. 13*A*, 13*B*, 14*F*–14*H*). Some subsidiary cells either are the same lengths as the guard cells (fig. 14*H*) or can extend beyond the guard cells on one polar side of the stoma (fig. 14*F*, 14*G*). Stomata are 30–48 μm long and 20–26 μm wide, and guard cells are 30–48 μm long and 6–9 μm wide. On the abaxial pinnule surface, SD is 68–75 per 1 mm^2, while the SI values, measured only over the intercostal field, vary from 8.5 to 9.3. This is markedly different from the SI and SD values for epidermal cells on the frond.

Stelar Anatomy

Anatomical preservation is restricted to the stems and branches, with most information gathered from five successive thin sections made from the paratype, which are spaced 1.5, 12, 12, and 1.5 mm apart (fig. 6*C*, a–e; fig. 15*A*–15*E*). Additional information was recovered from the lower and upper parts of the holotype, with slides made of sections 160 mm apart from each other (fig. 4*A*, f–i; fig. 15*F*–15*H*). Well-preserved tissues include primary and secondary xylem as well as the outer part of the cortex; parenchyma and phloem are imperfectly preserved.

Stems are eustelic and are composed of pith surrounded by axial bundles and leaf traces (fig. 16*A*–16*D*). The cortex is imperfectly preserved and is represented only by remains of thick-walled parenchyma cells. Pith appears to be roughly triangular in transverse section in the holotype (fig. 16*D*), with leaf trace bundles occupying the corners of the triangle (double arrows in fig. 16*D*). The pith in the stem of specimen PB23027 is extensively compressed, making determination of its original shape in transverse section problematic (fig. 16*A*–16*C*). Pith is represented only in transverse sections as a black area in the middle part of the stem (fig. 16*A*) and in longitudinal sections as small cells ca. 8 μm wide and ca. 60 μm long (p in fig. 17*J*, 17*L*). The poor preservation of this layer is in contrast to that of other well-preserved tissues, suggesting that it was probably parenchymatous.

Primary xylem is represented by axial bundles and leaf traces located at the margin of the pith (arrows, fig. 16*A*–16*D*). A maximum of eight bundles are present in transverse sections of the most complete stele (figs. 15*C*, 15*D*, 15*F*, 15*G*, 16*A*, 16*D*). However, more bundles may be present, as they are small and are often difficult to recognize, especially in areas of the stem with poor preservation and/or taphonomic compression. Individual bundles vary considerably in size (fig. 15). Leaf trace bundles are the most robust and are double stranded (fig. 17*B*, 17*D*, 17*H*). Bundles appear to be exarch, and some bundles show little or no development of centripetal/centrifugal metaxylem (fig. 17*A*).

PB23025. Scale bar = 200 μm. *I*, Detail of the double-stranded leaf trace zone. Primary xylem bundles are small and surrounded by protoxylem and metaxylem tracheids with mesarch development; arrow points to parenchyma cell zone with several small hidden intercalary spaces containing groups of small cells (arrowheads). Specimen PB23027. Scale bar = 50 μm. *J*, Longitudinal section showing metaxylem tracheids with scalariform thickening, large secondary xylem, and uniseriate ray cells (r). sx = secondary xylem; px = primary xylem; p = parenchyma cells of compressed pith surrounded on left side by secondary xylem (there is a missing primary xylem band) and on right side by metaxylem tracheids of primary xylem band in tangential section. Specimen PB23027. Scale bar = 50 μm. *K*, Detail of parenchyma cells of the outer cortex in transverse section. Specimen PB23027. Scale bar = 100 μm. *L*, Longitudinal section showing metaxylem tracheids with scalariform thickening, large secondary xylem with oval bordered pits on radial cell walls, and ray cells (arrow). sx = secondary xylem; px = primary xylem; p = parenchyma cells of compressed pith surrounded on both sides by metaxylem tracheids of the primary xylem band; r = ray cells. Radial view. Specimen PB23027. Scale bar = 50 μm.

This content downloaded from 147.188.216.059 on July 06, 2020 04:23:42 AM
All use subject to University of Chicago Press Terms and Conditions (http://www.journals.uchicago.edu/t-and-c).

In other areas, bundles are not fully preserved or are absent. Well-preserved leaf trace bundles are mesarch (fig. 17*B*, 17*D*). In transverse section, protoxylem cells are represented by small cells ca. 12–18 μm in diameter arranged around small parenchymatous "cores" (fig. 17*D*) or by cells lacking a core (fig. 17*H*). Sections with double-stranded leaf traces in the holotype show two strands of primary xylem bands, with cells lacking cores gathered together and surrounded by protoxylem and metaxylem tracheids (arrow, fig. 17*H*). These are more developed on the inside of the primary xylem bundles. The primary xylem core appears to have expanded in diameter during leaf trace departure. Protoxylem tracheids have not been observed in longitudinal section, so features of their wall thickenings are unknown. In transverse section, metaxylem tracheids are larger than protoxylem tracheids and are 25–50 μm in diameter. Metaxylem has scalariform thickenings in a tangential view of radial walls (px in fig. 17*J*, 17*L*).

Secondary xylem consists of alternating radial files of xylem and rays (fig. 17*A*). Files of tracheids are 4–12 cells wide in radial section and one to two cells wide in tangential section. In transverse section, tracheids are square to roughly rectangular and are up to 90 μm in diameter. Radial cell walls typically have three to five rows of alternate oval bordered pits (fig. 17*L*), but in the largest tracheids, there can be from two to seven rows. Xylem rays are typically uniseriate but are occasionally biseriate (fig. 17*J*). Individual rays are more than 3.5 mm high (fig. 16*E*). In tangential sections as well as radial sections, ray cells are angular and range from square to rectangular (figs. 16*E*, 17*J*, 17*L*), while in transverse sections, they are roughly rectangular, radially elongated, 30–60 μm long, and 8–15 μm wide (fig. 17*F*).

Occasionally a zone of thin-walled cells is preserved at the outer margin of the wood. This zone is approximately three cells wide and appears to represent a vascular cambium (arrow in fig. 17*H*). Fusiform initial cells are tangentially elongated and are 7 μm wide and ca. 40 μm long in transverse section (a in fig. 17*G*), while ray initials are 7 μm wide and 30 μm long in transverse section (b in fig. 17*G*). Secondary phloem has not been observed.

Cells of the cortex are very rarely preserved. Where present, the cortex comprises two zones of variable thickness that lack a sharp division. In transverse section, the inner cortex is 50–80 μm wide, while the outer cortex is 150–220 μm wide. The inner cortex comprises small cells that are 50–80 μm long and 13–25 μm wide and that are more or less tangentially elongated (fig. 17*C*, arrow). Cells in the outer cortex are larger, polygonal, and 30–90 μm in diameter (fig. 17*C*, 17*E*) in transverse section. In longitudinal section, they are roughly rectangular, 130–320 μm long (fig. 17*K*), and elongated parallel to the stem. Many cells are secretory, with dark or amber-colored contents (fig. 17*A*, 17*E*). The dark thin zone at the arrow in figure 17*E* appears to represent a periderm, but preserved cellular details are not present to allow this tissue to be further characterized.

As the anatomical preparations of the new plant came directly from specimens that had 3D morphological preservation and partial permineralization, anatomical features can be related to the branching organization of the plant as outlined above. Figure 15 presents successive sections from the paratype (PB23027) and holotype (PB23025), in both cases with the stem most probably showing axillary branching according to the specimens (see above). The most completely preserved sections from both specimens (fig. 15*C*, 15*G*, respectively, and fig. 16*A*, 16*D*) show three double-stranded leaf traces (numbered consecutively from bottom to top) and five single-stranded sympodia (labeled with roman numerals). Numbers of individual leaf traces start by the latest-formed leaves/fronds having the lowest numbers. Consequently, the numbering is used to construct a composite diagram of the vascular system for each specimen (fig. 15*J*, 15*K*).

Slides from the paratype specimen PB23027 represent five successive transverse sections through the stem (fig. 6*A*), spanning 27 mm through an internode. The lowermost transverse section, in figure 15*E*, is situated ca. 35 mm below the branch departure and shows a single preserved double-stranded leaf trace (1 in fig. 15*E*) on the left side. The sympodia on the right side of the same slide are not preserved. In figure 15*D*, 15*C*, it is possible to observe the progressive development in the size of leaf trace 1. Two primary vascular bundles appear to become more distant from each other (cf. fig. 15*E*, 15*C*). This leaf trace is not preserved in the uppermost sections (fig. 15*A*, 15*B*), as only the bottom half of the stem is present in these sections. Looking at the specimen slab, we conclude that this double leaf trace passes both of these sections (fig. 15*A*, 15*B*) and then enters the petiole situated under branch I* at the arrow in figure 6*C*. Detail of this leaf trace area in figure 15*C* shows parenchymatous cells (arrow, fig. 17*I*) of varying size, with several small, hidden intercalary spaces containing groups of small cells (arrowhead, fig. 17*I*) that are ca. 10–15 μm in transverse section. The small cells appear to represent primary xylem bundles entering the branch marked I* in figure 6*A*. These parenchyma cells, together with their small bundles, are situated between the pith and the leaf trace. Figure 15*C* shows the most completely preserved section (figs. 15*C*, 16*A*) and shows another two double-stranded leaf traces (numbered 2 and 3 in fig. 15*C* and at double arrows in fig. 16*A*). The leaf trace on the right side (2 in fig. 15*C*) is poorly preserved but appears to enter into the petiole from consecutive nodes situated above the branching point. The distance between figure 15*C* and the node situated above is 21.5 mm. Nevertheless, the PB23027 adpression specimen does not show a petiole attachment above this branching point for at least 50 mm. The progressive development of a leaf trace departing from the axial bundle is possibly observed in successive sections of the leaf trace situated in the middle part of the sections (3 in fig. 15). Figure 15*E* represents the point where this leaf trace separates from the axial bundle. In figure 15*C* (at a distance 13.5 mm from fig. 15*E*), those parts show an axial bundle separated from a double-stranded leaf trace; these are situated close to each other. In the uppermost figure 15*A*, 15*B*, two primary xylem bundles in the leaf trace are widely spaced, and the fascicle of secondary xylem consists of significantly smaller cells in transverse section. It appears that leaf trace 1 is separated tangentially from axial bundle I, leaf trace 2 from primary bundle III, and leaf trace 3 from primary bundle V (fig. 15*J*).

The most complete transverse sections of the holotype (figs. 15*G*, 16*C*) show a number of double-stranded and single-stranded bundles that are similar to those seen in specimen PB23027. Figure 15*F* and figure 15*G* come from internodes situated ca. 20 mm below the departing point of a branch and two fronds/leaves (see fig. 5*A*). Both sections show a large dark field in a middle part marked 1, which most probably represents a leaf trace and departing branch. Nevertheless, cellular composition of this area is unclear. On the basis of the combination of anatomical slides and adpression features, this "dark field" (a

This content downloaded from 147.188.216.059 on July 06, 2020 04:23:42 AM
All use subject to University of Chicago Press Terms and Conditions (http://www.journals.uchicago.edu/t-and-c).

in fig. 16*D*) appears to represent departing stem I** and a leaf base entering into the petiole situated near this branch (fig. 5*B*, II on the right side). Leaf trace 2 on the right side (2 in fig. 15*F*, 15*G*) of the transverse section is represented by petiole II, situated on the left side of figure 5*B*. The branch departs from the axil of a petiole situated on the right side, which corresponds to the presumable leaf traces in the dark field in figure 15*F*, 15*G*. Leaf trace 3 from figure 15*F* appears to represent the same leaf trace seen in figure 15*H* at a distance of 135 mm. The specimen slab shows only one branching zone (probably with two nodes). We believe that leaf trace 1 (fig. 15*F*) is departing from the node to the petiole (fig. 5*B*, marked II on the left side). The second leaf trace, 2 (fig. 15*F*), is departing to the petiole (together with the branch) from the next node, situated approximately 1.5 mm above the former node (fig. 5*B*, marked II on the right side). The third leaf trace, 3 (fig. 13*F*), passes both nodes. The transverse section (fig. 15*I*) of branch I** (fig. 5*B*) is only fragmental, with one leaf trace bundle. The thickness of the secondary xylem bundle is similar to that of the stem.

With only localized patches of anatomical preservation, the composite diagrams of the vascular system (fig. 15*J*, 15*K*) represent a fragmentary record of the stem's structure and include only two nodes and associated internodes from the holotype. Specimen PB23027 (fig. 15*J*) represents a case where leaf traces arise from the primary xylem axil bundle V, run alongside the cauline bundles for a short while, and divide again before reaching another node. The holotype shows double-stranded leaf traces where two depart from two closely arranged nodes, and a third passes both nodes and continues alongside the cauline bundles (fig. 15*K*). It is unclear how many nodes the double-stranded primary bundle passes before diverging into the petiole.

The aerial portions of the plant are reconstructed as a vine climbing on a *Cordaites* tree in figure 18.

Discussion

Comparisons and Affinity

Table 1 shows key features of Carboniferous/Permian plants that are most similar to those of the Wuda plant. Since the Wuda plant is a climbing plant, the following account largely focuses on climbing pteridosperms known from the late Carboniferous and early Permian of Euramerica. DiMichele at al. (2006) outlined several climbing or scrambling medullosan pteridosperms that were abundant in the Pennsylvanian and earliest Permian. Slender stems with axillary buds occur in *Medullosa endocentrica* Baxter, which, like the Wuda plant, was a vine (Hamer and Rothwell 1988). Like some pinnules in the Wuda plant, pinnules in *M. endocentrica* are well developed, but these are of the *Eusphenopteris* type (Baxter 1949; Hamer and Rothwell 1988) and are distinct from those of the Chinese plant. Significant differences occur in the size of the stems (23 mm in *M. endocentrica* and up to 4.5 mm in Wuda plant) and in the stem anatomy; the stele of *M. endocentrica* (Hamer and Rothwell 1988) comprises two to three vascular segments, as opposed to the single vascular segment in the Wuda plant. Petioles of *M. endocentrica* bifurcate, unlike those of the Wuda plant, which lack bifurcations (table 1). In addition, members of the Medullosales have much larger leaves and fronds (table 1). We conclude that the Wuda plant is not closely related to Medullosales.

Fig. 18 Reconstruction of the aerial parts of *Wudaeophyton wangii* sp. nov. (artist: Jiří Svoboda, under the guidance of J. Pšenička). A color version of this figure is available online.

Lyginopterid pteridosperms have reproductive organs on dichotomous branching systems (e.g., Hilton and Bateman 2006) rather than having them embedded in the leaf lamina, as appears to be the case in the Wuda vine. In lyginopterids, steles are eustelic or protostelic, with some species bearing pinnules of the

This content downloaded from 147.188.216.059 on July 06, 2020 04:23:42 AM
All use subject to University of Chicago Press Terms and Conditions (http://www.journals.uchicago.edu/t-and-c).

Table 1

Comparison of Key Features of Major Carboniferous and Permian Pteridosperm Groups

	Lyginopterids	Callistophytales	Medullosales	*Wudaeophyton wangii*
Stele	Singular vascular segment, eustelic or protostelic	Singular vascular segment, eustelic	Multiple vascular segments	Singular vascular segment, eustelic
Petiole	Mostly bifurcating but, very rarely, nonbifurcating	Bifurcating	Bifurcating	Nonbifurcating
Petiole surface character	Multicellular trichomes or multicellular capitate glands	Spinelike or glandular appendages	Naked before bifurcation or large lateral pinnules below the main fork of the frond	Prickles present
Leaf/frond	Small, up to 1 m in length, but 30 cm long in some species	Small, ca. 30 cm long	Large, up to 7–8 m long and 4 m wide	Small, 5–20 cm long
Reproductive organs	Dichotomous branching systems bearing small seeds and pollen organs; prepollen with trilete mark	Platyspermic ovules and pollen organs situated on lower side of pinnules; *Vesicaspora* pollen grain	Large seeds and pollen organs	Unknown

Rhodeopteridium type comparable to one of the pinnule forms in the Wuda plant. Climbing/scrambling lyginopterids from the late Carboniferous and early Permian include *Schopfiastrum decussatum* Andrews (Rothwell and Taylor 1972; Stidd and Phillips 1973; DiMichele at al. 2006), which was a climber with stems up to 30 mm wide. *Schopfiastrum decussatum* differs from the Wuda plant in being protostelic, in having abundant secondary xylem, and in having petiole traces that are distinctly abaxially toothed (Rothwell and Taylor 1972). According to Rothwell and Taylor (1972), fronds of *S. decussatum* were borne alternately and in two ranks, while in the Wuda plant, there is an axillary branching organization. Generally, lyginopterids have bifurcating petioles, except for *Microspermopteris* Baxter, which, like the Wuda plant, has a nonbifurcating petiole. *Microspermopteris* has a nearly solid protostele (Baxter 1952) that is very different from the eustele of the Wuda plant. *Heterangium* Corda is another small climbing/scrambling lyginopterid that bore *Rhodeopteridium*-type pinnules (Jennings 1976). However, *Heterangium* has a vitalized or mixed protostele (Taylor et al. 2009), which again differs from the eustele of the Wuda plant. We therefore do not consider the Wuda plant to be a member of the lyginopterids despite the fact that this group also includes climbers.

The combination of vegetative characters in the Wuda plant points to an affinity with or a close alliance with the Callistophytales (table 1), but without fertile organs, it is impossible to prove this. In particular, its climbing habit as a vine, its eustelic anatomy, and its leaf morphology, represented by pinnules with well-developed pinnule laminae, are very similar to those of members of the Callistophytales (Rothwell 1981). Because of the combination of preservation styles in the Wuda plant, we undertake comparisons with previously documented callistophytalean species preserved as both adpressions and permineralizations.

The primary vascular system of the Wuda plant consists of independent axial bundles or sympodia and leaf traces, as in species of *Callistophyton* (Rothwell 1975, 1981). There are two anatomically circumscribed species of *Callistophyton*, *C. boyssetii*, from the middle Pennsylvanian of North America, earliest Permian of Europe, and latest Permian of South China, and *C. poroxyloides*, from the late Pennsylvanian of North America (Rothwell 1981; Seyfullah and Hilton 2011). Systematically important similarities to both species of *Callistophyton* include a parenchymatous pith surrounded by five axil primary xylem bundles and leaf traces, secondary xylem composed of alternating files of tracheids and rays, and tracheids being angular and arranged in files of one to four cells (Rothwell 1975; table 2).

Although subtly different, the small hooked prickles on stems of the Wuda plant are easily homologized with the spinelike appendages of *C. boyssetii* (Rothwell 1975). Both *C. boyssetii* and the Wuda plant species also have cells with amber contents in the cortex (Rothwell 1975). However, differences include the fact that the Wuda plant lacks cells with amber contents in the pith and has mesarch xylem maturation, while in *C. boyssetii*, the pith has cells with amber contents, and xylem maturation is exarch (table 2). We consider the amber-colored cell contents to be taphonomically resistant; it is probable that these cells were absent in the pith of the Wuda plant rather than not preserved. Seyfullah et al. (2009) described a specimen of *C. boyssetii* from the latest Permian of South China with rays one to three cells wide that is distinct from both the Wuda plant, where rays are one or two cells wide, and from Euramerican *C. boyssetii*, where rays are one to four cells wide (Rothwell 1975; table 1). Seyfullah and Hilton (2011) speculated that this variation in ray cell organization could be related to the small size of the stem on the basis of which their observations were made; they inferred this to be a relatively immature part of the plant or a distal part of the stem. The stem from which anatomy was recovered for the Wuda plant comes from a specimen with large fronds/leaves attached directly to the stem together with one outgoing branch. From this, we conclude that, in the Wuda plant, rays that are one or two cells wide are not a consequence of being from a relatively immature or distal part of the plant and are thus reliable taxonomic characters that distinguish it from *C. boyssetii*. Other than this feature, the number of cells in individual rays is within the ranges declared for species of *Callistophyton* (Rothwell 1975).

Similarities also exist between *C. poroxyloides* and the Wuda callistophytalean (table 2); these similarities include mesarch xylem maturation, absence of amber-colored cell contents in the pith, and having two to seven rows of bordered pits in secondary

This content downloaded from 147.188.216.059 on July 06, 2020 04:23:42 AM
All use subject to University of Chicago Press Terms and Conditions (http://www.journals.uchicago.edu/t-and-c).

Table 2

Comparison of Key Features in Anatomically Preserved Callistophytalean Plant Species

	Callistophyton boyssetii	*Callistophyton poroxyloides*	*Johnhallia lacunosa*	*Wudaeophyton wangii*
Dimension of stem	2–30 mm;[a] ca. 10 mm[b]	2–30 mm	Up to 10 mm	2.5–4.5 mm
Xylem maturation	Exarch	Mesarch	Mesarch	Mesarch
No. primary xylem bundles	5	5	4	5
Leaf trace divergence	Tangential	Tangential	Radial	Tangential
Ray width	1–4 cells;[a] 1–3 cells[b]	1–4 cells	1 to several[c]	1–2 cells
Cells with amber-colored contents in cortex	Present	Absent	Absent	Present
Cells with amber-colored contents in pith	Present	Absent	Absent	Absent
Pinnule laminae development	Fully developed	Fully developed	Reduced/undeveloped	Heterophylly: fully developed and reduced/undeveloped
Spinelike appendages	Absent	Present	Absent	Present
Glandular appendages	Present	Absent	Absent	Absent
Pollen organs on abaxial surface of fertile pinnule	Present	Present	?	Present

[a] *Callistophyton boyssetii* from Euramerican flora.
[b] *Callistophyton boyssetii* from the latest Permian of China.
[c] According to Stidd and Phillips (1982), xylem rays are variable in height, ranging from low (one to three cells) to very high and composed of many cells.

tracheids. Differences include the fact that *C. poroxyloides* has glandular appendages, while these are absent in the Wuda plant, and that the Wuda plant has cells with amber-colored contents in the cortex, which are absent in *C. poroxyloides* (table 2). There is no doubt about the close relationship of the Wuda plant with the vegetative organs (especially the stem anatomy) of *Callistophyton*, but it is distinct from both *C. boyssetii* and *C. poroxyloides* (table 2). Importantly, key features in the diagnosis of *Callistophyton* are unknown in the Wuda plant, including indistinct cells of the pith, cortex, and secondary phloem, preventing it from being assigned to the genus. Rothwell (1975) also mentioned that leaf traces arise from divisions of sympodial bundles and run alongside the cauline bundles for two and a half nodes before dividing again. However, thin sections of specimen PB23027 demonstrate that a leaf trace divides rapidly to be double stranded within one internode in the Wuda plant (fig. 15*J*).

The Wuda plant shows great similarity to *Johnhallia lacunosa*, which is placed by some authors among the Callistophytales (Taylor et al. 2009). However, without any information about reproductive organs, its placement within the Callistophytales remains somewhat speculative. *Johnhallia* has eight primary xylem strands, of which five are axial and three are leaf traces, and it has *Rhodeopteridium*-type pinnules. Leaf traces in the Wuda plant occupy a space within the circle of the cauline bundles and diverge tangentially rather than diverging radially as they do in *J. lacunosa*. Stidd and Phillips (1982) outlined numerous other differences between *Johnhallia* and *Callistophyton*, including the presence of scalariform pitting in both protoxylem and metaxylem tracheids, several rows of oval bordered pits on radial and tangential sides of secondary xylem, and a series of transitional pitting types leading to tracheids with scalariform secondary wall thickenings present in *Johnhallia* and absent in *Callistophyton*. Unfortunately, in the Wuda plant, protoxylem tracheid thickenings have not been observed in longitudinal sections, with only rows of oval bordered pits noted on the radial side of the secondary xylem, similar to those of *Callistophyton* but absent in *Johnhallia*. In *Johnhallia*, the last divisions of the frond comprise two to four dichotomies in a single flattened plane, with the segments gradually diverging at small angles. These last flat divisions are delicate and lack internal cellular division into a palisade and spongy mesophyll; they appear to be of the *Rhodeopteridium* type and may be similar to those observed in the Wuda plant in pinnules with a reduced lamina.

On the basis of the discussion above, the Wuda plant shows considerable differences from lyginopterids and Medullosales (table 1) but much greater similarity to members of the Callistophytales and, in particular, *C. boyssetii*, *C. poroxyloides*, and *Johnhallia* (table 2). As the Wuda plant is distinct from these callistophytaleans, we establish *Wudaeophyton wangii* gen. et sp. nov. to accommodate this species. However, because the Wuda plant is represented only by vegetative organs, it is challenging to comprehensively assign it to a particular plant group, leading us to designate it as incertae sedis and, for the time being, consider it to be a probable member of the Callistophytales, until its reproductive organs are identified.

Comparison of Foliage

Pinnule forms of *W. wangii* show great variability, including pinnules of the *Pseudomariopteris-Emplectopteris* type that have fully developed pinnule laminae as well as transitional forms of the *Rhodeopteridium* type where the pinnule laminae are extremely reduced and are present only in the axils of midveins and lateral veins.

Pinnules with fully developed pinnule laminae of the *Pseudomariopteris* type occur in *Callistophyton*. Permineralized specimens of *C. boyssetii* with attached pinnules are rather narrowly attached and bluntly dentate, with a robust midvein that divides in an alternate fashion to produce more delicate laterals (Rothwell 1981). Although the pinnule shape is similar to that of

This content downloaded from 147.188.216.059 on July 06, 2020 04:23:42 AM
All use subject to University of Chicago Press Terms and Conditions (http://www.journals.uchicago.edu/t-and-c).

W. wangii, lateral veins divide several times in a short distance in *C. boyssetii* (Rothwell 1981), but in *W. wangii* they divide infrequently, typically dividing once or, very rarely, twice.

From the Pennsylvanian of Euramerica, the adpression foliage species *Dicksonites pluckenetii* (Schlotheim ex Sternberg) Sterzel, *D. sterzelii* Zeiller, and *Pseudomariopteris busquetti* have traditionally been assigned to the Callistophytales (Rothwell 1981; Krings and Kerp 2000; Krings et al. 2001; Galtier and Béthoux 2002). A major difference that *D. pluckenetii* and *P. busquetti* have from *Wudaeophyton* is the dichotomous nature of the petiole. While it is simple and undivided in *W. wangii*, *D. sterzelii* appears to have nonbipartite leaves (Galtier and Béthoux 2002), but the pinnatifid pinnules of *D. pluckenetii* and *D. sterzelii* have well-developed pinnule laminae with large, obtuse lobes (Galtier and Béthoux 2002), which are quite different from the pinnules that lack laminae with narrow and long lobes in *W. wangii*. While some similarities occur between the pinnule laminae of *W. wangii* and *D. pluckenetii* (e.g., fig. 9*A*), pinnule lobes are much larger in *Dicksonites* than in *Wudaeophyton* (Galtier and Béthoux 2002). Furthermore, the size of the petiole/secondary rachises is also notably different: 3–8 mm in diameter in *D. pluckenetii* (Galtier and Béthoux 2002) but only 1–2 mm in diameter in *Wudaeophyton*. Galtier and Béthoux (2002) also noted secretory glands on pinnules of *D. sterzelii*, whereas these are absent in *Wudaeophyton*.

Pseudomariopteris busquetti shares with *Wudaeophyton* fronds that are borne on the outgoing stem portion and are positioned almost in pairs, the presence of special features adapted for climbing (Krings and Kerp 2000; Krings et al. 2001), a large variation in frond/leaf size, and the presence of laminar pinnules. While petiole arrangement on the stem of *Wudaeophyton* could be described as being in "pseudo-pairs," we consider these to represent departures from two closely spaced nodes followed by a longer internode—this corresponds with similar observations of *P. busquetti* (Krings et al. 2001). Otherwise, petioles of *P. busquetti* are directed toward one side of the stem, while in *Wudaeophyton*, they are positioned on both sides and are organized oppositely. Pinnules of *P. busquetti* are characterized as variable in size and vary from tongue shaped to asymmetrically triangular and from entire margined to slightly lobed, and they are broadly attached, with a flexuous decurrent midvein and lateral veins that bifurcate two to four times (Krings and Kerp 2000). These features correspond well with those of some of the smaller pinnules of *Wudaeophyton* with fully developed pinnule laminae (e.g., fig. 10*C*). Nevertheless, the venation pattern is different in both species, with pinnules of *Wudaeophyton* having more or less straight midveins and lateral veins that dichotomize once or, rarely, twice. In contrast, pinnules of *P. busquetti* have a flexuous midvein, and lateral veins bifurcate two to four times. Another significant difference between these species is the presence of pinnules with extremely reduced laminae in *Wudaeophyton*, while in *P. busquetti*, all pinnules consistently have well-developed laminae. The major differences between both species are in their different adaptations for climbing. *Pseudomariopteris busquetti* has climber hooks in the distal region of ultimate pinnae in fronds situated in the distal part of the plant, while in *W. wangii*, pinnule climbing adaptations are terminated by pads, and stems have small hooked prickles.

Some similarities to pinnules with fully developed pinnule laminae can also be observed in species of climbing lyginopterids, including *Mariopteris* Zeiller, *Karinopteris* Boersma, and *Helenopteris* Krings and Kerp. The major difference between these genera and *Wudaeophyton* is the character of their fronds, which bear only pinnules with fully developed pinnule laminae in *Mariopteris*, *Karinopteris*, and *Helenopteris*, while *Wudaeophyton* is strongly heterophyllous, with *Pseudomariopteris-Emplectopteris*–type and *Rhodeopteridium*-type pinnules in nonbipartite fronds.

Pinnules with fully developed pinnule laminae in *Wudaeophyton* are similar to those of *Emplectopteris triangularis* Halle (Halle 1927) from the Shihhotse Formation of North China, which has also been interpreted as a member of the Callistophytales (Seyfullah and Hilton 2009, 2011). Both *E. triangularis* and *Wudaeophyton* have ultimate pinnae that are alternate or subopposite on the penultimate rachis and have more or less triangular pinnules (Seyfullah and Hilton 2009). Pinnules of *E. triangularis* have a weakly anastomosing venation pattern, and many distal parts of the penultimate pinnae bear intercalated pinnules on the rachis between the ultimate pinnae (Seyfullah and Hilton 2009). Another difference is the presence of frequent small glands on the rachis and pinnules of *E. triangularis*; these are absent in *Wudaeophyton*.

In *Wudaeophyton*, liana-like pinnule climbing adaptations are present on some pinnules (e.g., fig. 11*G*). These are very similar to specialized climbing organs previously described in the Pennsylvanian pteridosperm *Blanzyopteris praedentata* (Gothan) Krings and Kerp (Krings and Kerp 1999). In *B. praedentata*, fronds are borne in subopposite pairs, with one member of a pair highly modified with branchlets terminating in adhesive pads. The adhesive pads in *B. praedentata* occur on highly modified leaves/fronds bearing densely organized trichomatous tubes, with tubes of the last order terminated by adhesive pads (Krings and Kerp 1999). Krings and Kerp (1999) also described different specialized cells situated where the tubes start to widen. These cells are significantly wider than they are high, especially on the interior surface, and have strongly cutinized transverse anticlinal walls (Krings and Kerp 1999). These cells are similar but not identical to the small cells also creating a ring under adhesive pads that occur in *Wudaeophyton*, although in *Wudaeophyton*, they are high rather than wid and are more difficult to fully characterize because of preservational limitations. While these climbing structures are subtly different from each other, they both function to attach the plant during climbing.

Adhesive pads are also known from several extant vine-like plants, including species of *Parthenocissus* (Junker 1976; He et al. 2008). Tendrils of living *Parthenocissus tricuspidata* hold the plant and provide strong mechanical support for the vine. According to He et al. (2008), many spongelike structures and vessels are situated inside each pad, helping to carry and accumulate chemical substances secreted by the plant, which in turn increases adhesiveness. Accumulation of adhesives within the pad cells is documented in *Wudaeophyton* in figure 11*J*. Large fronds/leaves of *Wudaeophyton* bearing only these specialized laminae with pinnule climbing adaptations functioned as a tool for fixing the plant on relatively smooth stems. As mentioned by Krings and Kerp (1999), the zone of specialized cells just below the adhesive pad may have functioned as a shock absorber, absorbing movement from wind that could have a potentially large effect in higher and more exposed climbing positions. These features supported the idea that *Wudaeophyton* as a climber could

This content downloaded from 147.188.216.059 on July 06, 2020 04:23:42 AM
All use subject to University of Chicago Press Terms and Conditions (http://www.journals.uchicago.edu/t-and-c).

reach the treetops in the Wuda forest, growing on *Cordaites* trees. This is further supported by the common association of *Wudaeophyton* and *Cordaites* leaves and branches in the studied locality (fig. 2).

Comparisons of Reproductive Organs

Comparison of the reproductive organs of *W. wangii* gen. et sp. nov. is difficult, as the only evidence about them comes from impressions of the former attachment sites embedded into laminate pinnules. We consider these structures to be the remains of attached fertile organs that are not preserved. In *W. wangii*, such impressions occur on the lower (abaxial) surface of lobate pinnules with fully developed pinnule laminae (fig. 12*B*), with the fertile organs appearing to be connected to the vascular system between the midvein and pinnule margin. Synangial pollen organs and ovules of *Callistophyton* are borne on the lower side of pinnules (Rothwell 1980) and are attached to the pinnule by a vascular strand (Rothwell 1981). In male pinnules of *Callistophyton*, a pad of vascular tissue occurs at the junction of the vascular tissue and the synangia, and this is most likely what the preserved structures in *Wudaeophyton* are rather than part of the synangia themselves. We consider it unlikely that the symmetrical shape of the fertile organs in *Wudaeophyton* had bilaterally symmetrical cardiocarpalean-type ovules attached as seen in species of *Callistophyton* that bear ovules of *Callospermarion* (Rothwell 1981; Hilton et al. 2002).

The laminar type of pinnules in *Wudaeophyton* is similar to the ovule-bearing foliage of *Norinosperma shanxiensis* Seyfullah and Hilton, from Taiyuan Formation in North China (Seyfullah and Hilton 2009). Both species bear pinnules that are subalternate or subopposite, with fully developed pinnule laminae that are unevenly lobed and entire. Nevertheless, the venation pattern and character of pinnule lobes appear to be slightly different in each species. According to Seyfullah and Hilton (2009), pinnules of *Norinosperma shanxiensis* have acutely angled pinnule lobes with a straight midvein and lateral veins that dichotomize several times. *Wudaeophyton* has a simpler venation pattern where lateral veins dichotomize once or, very rarely, twice, and laminate pinnules have blunt lobes. The ovule-bearing pinnules of *Wudaeophyton* are at present unknown.

In addition to the ovule-bearing species *Norinosperma shanxiensis*, Seyfullah and Hilton (2009) also described the fertile male pinnule *Norinotheca shanxiensis*, concluding that they most likely belonged to the same whole plant species. *Norinotheca shanxiensis* and *Wudaeophyton* are similar in the laminar character of their small pinnules, having a simple venation pattern where relatively thick lateral veins are undivided, and reductive organs occur on the lower pinnule surface between the midvein and the margin. Both species also have large attachment points where the fertile organs are embedded into the pinnule (compare Seyfullah and Hilton [2009], fig. 41, with fig. 12*C*, 12*E*). Nevertheless, significant differences exist between them. Pinnules of *Norinotheca shanxiensis* have confluent bases, the penultimate rachis appears to be winged, and synangia are placed underneath the secondary vein. In *Wudaeophyton*, pinnules are free, although they can be closely arranged, and reproductive organs are attached to the end of lateral veins that terminate in the middle of the midvein and pinnule margin. It is clear that *Norinotheca shanxiensis* and *Wudaeophyton* represent two different biological species from the Taiyuan Formation. From this evidence, we consider it likely that the Taiyuan Formation contains at least three different kinds of callistophytalean plant (table 3), the *Norinosperma*/*Norinotheca* plant, the plant bearing *Callospermarion* ovules in coal ball assemblages, and probably *Wudaeophyton*.

Reconstruction of Wudaeophyton

The habit of *W. wangii* gen. et sp. nov. is illustrated in figure 18 on the basis of a synthesis of the evidence presented in the description. The aerial part of the plant is represented by ca. 3–4-mm-wide stems that are occasionally branched and bear variably sized leaves/fronds attached in nodes. It is unlikely that stems of this diameter were self-supporting, and their pinnule climbing adaptations imply a climbing liana-like habit as a vine. We consider it to be vine- and liana-like rather than a trueliana, as extant lianas have vessels that allow low resistance to water flow (e.g., Rowe and Speck 1998; Kozlowski and Pallardy 2002; Masselter et al. 2007). Vessel elements are absent in *Wudaeophyton* and other members of the Callistophytales. Branching is axillary, documented mainly from two specimens (holotype PB23025 and PB23027), with both specimens showing that long sections of the widest stems are over 200 mm (denoted as stem I on plates) with only one very short branching zone (fig. 4*B*, nodes, and fig. 6*A*, frame). Branches are situated in the axil of the stem and the petiole. The holotype (PB23025) shows a petiole outgoing from an area where closely situated nodes occur at a distance of 1.5 mm apart (fig. 5*A*, 5*B*).

By contrast, the node on the stem of specimen PB23027 (fig. 6*A*, frame) has just one outgoing petiole, with no other nodes positioned for at least 50 mm from the node proximally or distally. A similar situation is presented on another branch of the holotype (fig. 4*B*, denoted as I**, enlarged in fig. 5*D*), where the distance between two nodes is 15 mm. Nodal frequency appears to vary along the stem, with stems having zones with long and short internodes. The shortest internodes (millimeters apart) are in the zone where the branch departs from the stem, and short internodes occur in the proximal part of branches, while longer internodes occur distally. This style of branching resembles that of some extant climbing angiosperms, such as *Wisteria sinensis*.

Petioles of bipinnate fronds/leaves arise at a nearly right angle from slightly swollen nodes on the stem (fig. 5*D*). They are pinnately compound and fernlike, but there is considerable variation in both frond size and character depending on their position on the plant as well their function and stage of development. Although entire fronds/leaves were not discovered, large parts are preserved in specimens PB23025 (holotype), PB23026, PB23032, and PB23033. They represent a range of different pinnule types in terms of their size and pinnule composition. The smallest fronds/leaves were a few centimeters long (figs. 5*C*, II, 9*B*), while large ones were ca. 200 mm long (fig. 5*L*). In *Wudaeophyton*, three major frond/leaf morphologies exist (see above), but many transitional forms are also present. Generally, large fronds/leaves, which bear pinnules with pinnule climbing adaptations and have reduced pinnule laminae in most pinnules, are attached to the widest stems and represent the proximal

This content downloaded from 147.188.216.059 on July 06, 2020 04:23:42 AM
All use subject to University of Chicago Press Terms and Conditions (http://www.journals.uchicago.edu/t-and-c).

Table 3

Callistophytalean Fossils and the *Wudaeophyton wangii* Plant from Euramerican and Cathaysian Floras

	Euramerican flora		Cathaysian flora		
	North America and Europe, Middle Pennsylvanian (Carboniferous) to earliest Permian (Asselian)	Only North America, Upper Pennsylvanian (Carboniferous)	Taiyuan Formation, North China, Asselian, Cisuralian (Early Permian)	Lower Shihhotse Formation, North China, Kungurian to Wordian stages, Guadalupian (middle Permian)	Xuanwei Formation, South China, Wuchiapingian Stage, Lopingian (upper Permian)
Callistophyton boyssetii plant:					
Stems: *C. boyssetii*	Present				Present
Leaves: *Dicksonites pluckenetii* type	Present				
Ovules: *Callospermarion undulatum*	Present		Present		
Pollen organs: *Idanothekion glandulosum*	Present				
Pollen: *Vesicaspora*	Present[a]	Present[a]	Present	Present[a]	Present[a]
Callistophyton poroxyloides plant:					
Stems: *C. poroxyloides*		Present			
Leaves: unknown					
Ovules: *Callospermarion pusillum*		Present			
Pollen organs: *Idanothekion callistophytoides*		Present			
Pollen: *Vesicaspora*		Present[a]	Present	Present[a]	Present[a]
W. wangii plant:					
Stems: *W. wangii*			Present		
Leaves: *Rhodeopteridium* type	Present		Present		
Ovules: unknown					
Pollen organs: unknown					
Pseudomariopteris busquetii	Present				
D. plukenetii	Present				
Norinotheca shanxiensis (male fertile frond)			Present		
Norinosperma shanxiensis (female fertile frond)			Present		
Emplectopteris triangularis (female fertile frond)				Present	

[a] Pollen could be produced by either species of *Callistophyton* but may also have been produced by other members of the Callistophytales (see text for discussion).

This content downloaded from 147.188.216.059 on July 06, 2020 04:23:42 AM
All use subject to University of Chicago Press Terms and Conditions (http://www.journals.uchicago.edu/t-and-c).

part of the stem. Smaller fronds/leaves are, by contrast, situated on the proximal part of stems/branches and are probably also on branches departing from the stem. The smallest type stands on the most proximal part of branches. All fronds/leaves show significant asymmetry on the basis of the distal parts of the specimens figured in figure 6*E*–6*G* and the characters of fronds/leaves in specimen PB23026 (fig. 7*B*). The precise frond/leaf shape is not identifiable because nearly all of the ultimate pinnae, which can define the outline of the frond, are incompletely preserved. A lanceolate shape for the fronds/leaves is estimated on the basis of specimens PB23033, PB23025 (holotype), and PB23040. These examples show shorter ultimate pinnae situated in the proximal parts of fronds/leaves in comparison with longer ultimate pinnae in the middle and ultimate parts of fronds/leaves. Specimen PB23040 represents the lowermost part of a frond/leaf, ca. 30 mm from its point of attachment to the stem, and the length of these two opposite ultimate pinnae is ca. 15 mm.

The liana-like habit of *W. wangii* is supported by six lines of evidence, namely: (1) Remains of *W. wangii* are absent in the lowermost part of the in situ tuff horizon (fig. 2), showing that it was not growing on the forest floor or understory and did not have a ground-dwelling scrambling habit. (2) It bears strong adhesive pinnule climbing adaptations that allowed the plant to gain support and to climb to higher stories of the forest. (3) It has a relatively thin stem that is rarely straight and appears to have been flexible. (4) It has hooked prickles that allowed it to climb and attach itself to a supported plant. (5) Paleoecological associations demonstrate that *Wudaeophyton* co-occurs with cordaitalean branches and *Psaronius* fronds that were part of the forest canopy preserved in the upper part of the volcanic tuff horizon (fig. 2). Within Callistophytales, previous reconstructions of *Callistophyton* (Rothwell 1975, 1981) and *D. pluckenetii* (Galtier and Béthoux 2002) demonstrated them to be small shrubby plants with scrambling stems. However, the reconstruction of *W. wangii* is more similar to the reconstruction of *P. busquetii* published by Krings et al. (2001), which has a liana-like habit as a vine.

Ecology

During the Permian, the Cathaysian paleofloristic realm extended up to ~30° north. Existing paleoclimatic models for the Permian indicate that North China was principally a tropical province (Rees et al. 2002; Ziegler et al. 2003). Here we interpret *Wudaeophyton* to represent a callistophytalean vine and consider it to be an integral part of the peat-forming forest community. DiMichele et al. (2006) summarized the ecology of callistophytaleans, considering them to be opportunists characterized by wind pollination, production of many small seeds, patchy occurrence within wetland landscapes, and focus on the colonization of available physical space in the forest (DiMichele et al. 2006). As developed here, *Wudaeophyton* was adapted for an ecological niche in the canopy of the peat-forming forest community among the trunks and branches in the upper forest story, which was also the interpretation for *P. busquetii* (Krings et al. 2001).

During fieldwork to sample the Wuda tuff peat-forming flora comprising forests dominated by the cordaitalean tree fern as well as the sigillarian *Paratingia*, in a study area exceeding 2000 m^2, only 64 specimens of *Wudaeophyton* have been discovered. In several excavations within the Wuda exposures, *Wudaeophyton* remains had accumulated in the upper part of the in situ volcanic ash horizon, where 87.3% of specimens of *Wudaeophyton* occur (fig. 2). Specimens of *Wudaeophyton* are exclusively associated with cordaitalean leaves in the uppermost part of the ash horizon and with *Psaronius* fronds in the middle and upper parts of the ash horizon. There is no evidence of *Wudaeophyton* in the lowermost part of the ash horizon, suggesting that it did not have a scrambling life strategy. This suggests that *Wudaeophyton* did not colonize available physical space on the forest floor but does suggest that it exclusively inhabited the highest trees in the forest community, climbing on *Cordaites* and *Psaronius* trees in cordaitalean tree fern forest settings. Strong fixing methods to support the plant, including adhesive pads, can explain why only several plant fragments of this species were discovered at this locality. Specimens of *Wudeaophyton* could have remained attached to upright stems a long time after the primary ashfall event occurred, with dead stems protruding from the volcanoclastic sediment. They probably decomposed directly on their supporting plants and did not fall into the ash to be incorporated into the sediment for preservation. Only parts of *Wudaeophyton* that were attached to the branches of cordaitaleans or to not so solidly supported plants, like the frond rachises of *Psaronius*-type trees, were able to enter into the fossil record. This difficulty in going into the fossil record may explain why *Wudaeophyton* has not been found at other localities or on other canopy trees, such as *Sigillaria*. Therefore, the volcanic eruption causing the ashfall event facilitated a unique set of circumstances that preserved plants not preserved elsewhere.

An interesting factor for environmental interpretations of *W. wangii* is its low vein density and reduced leaf laminae in comparison with *Callistophyton*. DiMichele et al. (2006) considered that a lower vein density could be an indication of growth under drier conditions through reduction of water loss. Contrary to this, xerophytic characters may occur in plants in ever-wet habitats, including peat-accumulating and clastic swampy settings (Potonié 1913; Cleal and Shute 2012; Stull et al. 2012), and cannot be considered to be direct indicators of real drier habitats. In this context, xerophytic characters of plants that are adapted to extremely dry settings may alternatively reflect the very low nutrition values of the substrate.

Strong heterophylly in *W. wangii* supports the idea of its liana-like character because that is a conspicuous feature of many extant climbing plants (Cremers 1973, 1974; Lee and Richards 1991; Burnham 2009). It is very difficult to say whether the heterophylly of *W. wangii* is an expression of heteroblastic development or a programmed ontogenetic change in morphology (Steeves and Sussex 1989; Winn 1999). Small laminate pinnules bearing reproductive organs can point to homoblastic development, where pinnules with fully developed pinnule laminae represent the male- or female-bearing organs. These questions remain open and will require additional specimens for further evaluation.

Species Concepts and Evolutionary and Floristic Implications

We interpret *Wudaeophyton* as adding to the pteridosperm diversity of the early Permian Taiyuan Formation (table 3). Callistophytales in this formation also include permineralized ovules of *Callospermarion undulatum* in coal balls (Hilton et al.

This content downloaded from 147.188.216.059 on July 06, 2020 04:23:42 AM
All use subject to University of Chicago Press Terms and Conditions (http://www.journals.uchicago.edu/t-and-c).

2002) and fertile fronds of *Norinosperma* (ovulate) and *Norinotheca* (synangial) in compression/impression assemblages (Seyfullah and Hilton 2009), with *Norinosperma* and *Norinotheca* presumably belonging to a single whole plant species. The Taiyuan Formation also contains pollen grains of *Vesicaspora* (Ouyang et al. 2017) produced by both species of *Callistophyton* (Rothwell 1981), although it is unknown whether other members of the Callistophytales also had the same kind of pollen; presence of *Vesicaspora* is not necessarily an indicator of the presence of species of *Callistophyton* in the Taiyuan Formation. As presently characterized, the *C. boyssetii* whole plant bears ovules of the *C. undulatum* type (Rothwell 1981), suggesting that *C. boyssetii* is also present. This remains speculative, as it is unclear whether different whole plant species within the Callistophytales bore the same kind of ovule (see Bateman and Hilton 2009). Ovules are presently unknown in *Wudaeophyton*, while *Norinosperma* lacks the anatomical preservation that would allow its ovules to be related to permineralized ovule species; it is therefore unclear whether neither, one, or both of these species bore anatomically preserved ovules of *C. undulatum*. The presence of *C. boyssetii* in the Lopingian (late Permian) of South China (Seyfullah and Hilton 2009; Seyfullah et al. 2009) suggests that other parts of the same whole plant species, including ovules of *C. undulatum* and pollen organs of *Idanothekion glandulosum*, may also be present in the Xuanwei Formation.

On the basis of stratigraphic occurrences of Callistophytales in the Euramerican and Cathaysian floras, it appears that the family originated during the middle Pennsylvanian in peat-forming wetlands of Europe and North America. The group diversified slowly in Euramerica during the middle-upper Pennsylvanian and migrated into North China during the latest Pennsylvanian alongside other wetland plant species (Hilton and Cleal 2007). Within Euramerica, the group experienced regional extirpation broadly coincident with the Carboniferous-Permian boundary (Hilton et al. 2002; Hilton and Cleal 2007; Seyfullah and Hilton 2011), but within Cathaysia it continued throughout most of the Permian. Within the Permian Cathaysian floras, Callistophytales include species that extended their stratigraphic and geographic ranges from the Pennsylvanian of North America and Europe after their Euramerican extirpation, as well as endemic species that show that the group also diversified at that time. Species persisting from the Pennsylvanian of Euramerica include *C. undulatum* in the Taiyuan Formation of North China (Hilton et al. 2002) and stems of *C. boyssetii* from the Lopingian-aged (late Permian) Xuanwei Formation of South China (Seyfullah et. al. 2009). Endemic Cathaysian species include *Wudaeophyton*, *Norinosperma*, and *Norinotheca* from the Taiyuan Formation and *E. triangularis* from the Guadalupian-aged (mid-Permian) Lower Shihhotse Formation, which shows that the family diversified within Cathaysia after its Pennsylvanian Euramerican acme. *Vesicaspora* occurs throughout the Permian of North China from the Taiyuan Formation onward, suggesting that members of the Callistophytales were widespread in this region (Ouyang et al. 2017). On the basis of macrofossil evidence, it appears that the group became extinct before the Triassic, with its youngest stratigraphical occurrence being *C. boyssetii* from the early part of the Xuanwei Formation in South China (Seyfullah et al. 2009; Seyfullah and Hilton 2011). Callistophytales are absent in latest Permian coal balls from the Wangjiazhai Formation in South China (Tian and Zhang 1980; Wang et al. 2009), suggesting that they went extinct before the end-Permian mass extinction event.

Acknowledgments

Funding was provided by the National Natural Science Foundation of China (grants 41530101, 41802011), the Strategic Priority Research Program (B) of the Chinese Academy of Sciences (XDB18000000, XDB26000000), a Visiting Professorship for Senior International Scientists of the Chinese Academy of Sciences (2016vea004), the Grant Agency of the Czech Republic (grant project 19-06728S), and the Research Program of the Institute of Geology AS CR, v.v.i. (RVO67985831). We thank František Tichávek (West Bohemia Museum, Pilsen) for making the thin sections, M. Mazuch and Mao Mao Yongqiang for assistance with scanning electron microscopy analysis, and Jiří Svoboda for drawing the reconstruction of the plant. Finally, we would like to thank Gar Rothwell and an anonymous reviewer for their help and constructive comments.

Literature Cited

Bateman RM, J Hilton 2009 Palaeobotanical systematics for the phylogenetic age: applying organspecies, formspecies and phylogenetic species concepts in a framework of reconstructed fossil and extant wholeplants. Taxon 58:1254–1280.

Baxter RW 1949 Some pteridospermous stems and fructifications with particular reference to the Medullosae. Ann Mo Bot Gard 36:287–352.

——— 1952 The Coal Age flora of Kansas. 1. *Microspermopteris aphyllum* var. *kansensis*, var. nov. Trans Kans Acad Sci 55:101–103.

Burnham R 2009 An overview of the fossil record of climbers: bejucos, sogas, trepadoras, lianas, cipós, and vines. Rev Bras Paleontol 12:149–160.

Cleal CJ, CH Shute 2012 The systematic and palaeoecological value of foliage anatomy in Late Palaeozoic medullosalean seed-plants. J Syst Palaeontol 10:765–800.

Cohen KM, S Finney, PL Gibbard, JX Fan 2013 (updated 2017) The ICS international chronostratigraphic chart. Episodes 36:199–204.

Cremers G 1973 Architecture de quelques lianes d'Afrique tropicale. I. Candollea 28:249–280.

——— 1974 Architecture de quelques lianes d'Afrique tropicale. II. Candollea 29:57–110.

DiMichele WA, TL Phillips, HW Pfefferkorn 2006 Paleoecology of Late Paleozoic pteridosperms from tropical Euramerica. J Torrey Bot Soc 133:83–118.

Fairon-Demaret M, J Hilton, CM Berry 1999 Surface preparation of macrofossils: dégagement. Pages 33–35 *in* TP Jones, NP Rowe, eds. Fossil plants and spores: modern techniques. Geological Society of London, London.

Galtier J, O Béthoux 2002 Morphology and growth habit of *Dicksonites pluckenetii* from the Upper Carboniferous of Graissessac (France). Geobios 35:525–535.

Gentry AH 1991 The distribution and evolution of climbing plants. Pages 3–49 *in* FE Putz, HA Moody, eds. The biology of vines. Cambridge University Press, Cambridge.

Halle TG 1927 Palaeozoic plants from central Shansi. Palaeontol Sin 2:1–316.

This content downloaded from 147.188.216.059 on July 06, 2020 04:23:42 AM
All use subject to University of Chicago Press Terms and Conditions (http://www.journals.uchicago.edu/t-and-c).

Hamer JJ, GW Rothwell 1988 The vegetative structure of *Medullosa endocentrica* (Pteridospermopsida). Can J Bot 66:375–387.

He TX, WW Yang, WL Deng 2008 A climbing plant with super-adhesive function advances and new results of the most recent study on *Parthenocissus tricuspidata*. Prog Nat Sci 18:1220–1225. (In Chinese.)

Hilton J, RM Bateman 2006 Pteridosperms are the backbone of seed-plant phylogeny. J Torrey Bot Soc 133:119–168.

Hilton J, CJ Cleal 2007 The relationship between Euramerican and Cathaysian tropical floras in the Late Palaeozoic: palaeobiogeographical and palaeogeographical implications. Earth Sci Rev 85:85–116.

Hilton J, SJ Wang, WQ Zhu, B Tian, J Galtier, AH Wei 2002 *Callospermarion* ovules from the Early Permian of northern China: palaeofloristic and palaeogeographic significance of callistophytalean seed-ferns in the Cathaysian flora. Rev Palaeobot Palynol 120:301–314.

Jennings JR 1976 The morphology and relationships of *Rhodea*, *Telangium*, *Telangiopsis*, and *Heterangium*. Am J Bot 63:1119–1133.

Junker S 1976 A scanning electron microscopic study on the development of tendrils of *Parthenocissus tricuspidata* Sieb. and Zucc. New Phytol 77:741–746.

Kozlowski TT, SG Pallardy 2002 Acclimation and adaptive responses of woody plants to environmental stresses. Bot Rev 68:270–334.

Krings M, H Kerp 1999 Morphology, growth habit and ecology of *Blanzyopteris praedentata* (Gothan) nov. comb., a climbing neuropteroid seed fern from the Stephanian of central France. Int J Plant Sci 160:603–619.

——— 2000 A contribution to the knowledge of the pteridosperm genera *Pseudomariopteris* Danze-Corsin nov. emend. and *Helenopteris* nov. gen. Rev Palaeobot Palynol 111:145–195.

Krings M, H Kerp, EL Taylor, TN Taylor 2001 Reconstruction of *Pseudomariopteris busquetti*, a vine-like Carboniferous–Early Permian pteridosperm. Am J Bot 88:767–776.

——— 2003 How Paleozoic vines and lianas got off the ground: on scrambling and climbing Carboniferous and Early Permian pteridosperms. Bot Rev 69:204–224.

Lee DW, JH Richards 1991 Heteroblastic development in vines. Pages 205–243 *in* FE Putz, HA Mooney, eds. The biology of vines. Cambridge University Press, Cambridge.

Li H, DW Taylor 1998 *Aculeovinea yunguiensis* gen. et sp. nov., a new taxon of gigantopterid axis from the Upper Permian of Guizhou Province, China. Int J Plant Sci 159:1023–1033.

——— 1999 Vessel-bearing stems of *Vasovinea tianii* gen. et sp. nov. (Glossopteridales) from the Upper Permian of Guizhou Province, China. Am J Bot 86:1563–1575.

Li H, BL Tian, EL Taylor, TN Taylor 1994 Foliar anatomy of *Gigantonoclea guizhouensis* (Gigantopteridales) from the Upper Permian of Guizhou Province, China. Am J Bot 81:678–689.

Masselter T, NP Rowe, T Speck 2007 Biomechanical reconstruction of the Carboniferous seed fern *Lyginopteris oldhamia*: implications for growth form reconstruction and habit. Int J Plant Sci 168:1177–1189.

Opluštil S, J Wang, HW Pfefferkorn, J Bek, J Pšenička, M Libertín, SJ Wang, et al Forthcoming Early Permian coal-forest preserved *in situ* in volcanic ash bed in the Wuda Coalfield, Inner Mongolia, China. Rev Palaeobot Palynol.

Ouyang S, CL Lu, HC Zhu, F Liu 2017 The Late Palaeozoic spores and pollen of China. University of Science and Technology of China Press, Hefei. 1092 pp.

Pfefferkorn HW, J Wang 2007 Early Permian coal-forming floras preserved as compressions from the Wuda District (Inner Mongolia, China). Int J Coal Geol 69:90–102.

Potonié R 1913 Über die xerophilen merkmale der pflanzen feuchter standorte. Sitz Ges Natforsch Freunde Berl 453–475.

Rees PM, AM Ziegler, MT Gibbs, JE Kutzbach, PJ Behling, DB Rowley 2002 Permian phytogeographic patterns and climate data/model comparisons. J Geol 110:1–31.

Rothwell GW 1975 The Callistophytaceae (Pteridospermopsida). I. Vegetative structures. Palaeontogr Abt B 151:171–196.

——— 1980 The Callistophytaceae (Pteridospermopsida). II. Reproductive features. Palaeontogr Abt B 173:85–106.

——— 1981 The Callistophytales (Pteridospermopsida): reproductively sophisticated Paleozoic gymnosperms. Rev Palaeobot Palynol 32:103–112.

Rothwell GW, TN Taylor 1972 Carboniferous pteridosperm studies: morphology and anatomy of *Schopfiastrum decussatum*. Can J Bot 50:2649–2658.

Rowe NP, T Speck 1998 Biomechanics of plant growth forms: the trouble with fossil plants. Rev Palaeobot Palynol 102:42–63.

Seyfullah LJ, J Hilton 2009 Re-evaluation of Halle's fertile pteridosperms from the Permian floras of Shanxi Province, China. Plant Syst Evol 279:191–218.

——— 2011 Callistophytalean pteridosperms from Permian aged floras of China. Palaeontology 54:287–302.

Seyfullah LJ, J Hilton, SJ Wang, J Galtier 2009 Anatomically preserved pteridosperm stems and petioles from the Permian floras of China. Int J Plant Sci 170:814–828.

Smith AR, KM Pryer, E Schuettpelz, P Korall, H Schneider, PG Wol 2006 Classification for extant ferns. Taxon 55:705–731.

Steeves TA, IM Sussex 1989 Patterns in plant development. 2nd ed. Cambridge University Press, Cambridge.

Stidd BM, TL Phillips 1973 The vegetative anatomy of *Schopfiastrum decussatum* from the Middle Pennsylvanian of the Illinois Basin. Am J Bot 60:463–474.

——— 1982 *Johnhallia lacunosa* gen. et sp. n.: a new pteridosperm from the Middle Pennsylvanian of Indiana. J Paleontol 56:1093–1102.

Stull GW, WA DiMichele, H Falcon-Lang, WJ Nelson, S Elrick 2012 Palaeoecology of *Macroneuropteris scheuchzeri*, and its implications for resolving the paradox of "xeromorphic" plants in Pennsylvanian wetlands. Palaeogeogr Palaeoclimatol Palaeoecol 331/332:162–176.

Taylor TN, EL Taylor, M Krings 2009 Paleobotany: the biology and evolution of fossil plants. Academic Press, New York. 1230 pp.

Tian BL, LW Zhang 1980 Fossil atlas of Wangjiazhai mine region in Suicheng, Guizhou. China Coal Industry Publishing House, Beijing. (In Chinese.)

Wang J, HW Pfefferkorn 2013 The Carboniferous–Permian transition on the North China microcontinent: oceanic climate in the tropics. Int J Coal Geol 119:106–113.

Wang J, HW Pfefferkorn, Y Zhang, Z Feng 2012 Permian vegetational Pompeii from Inner Mongolia and its implications for landscape paleoecology and paleobiogeography of Cathaysia. Proc Natl Acad Sci USA 109:4927–4932.

Wang SJ, KQ Sun, JZ Cui, SM Ma 2009 Fossil plants from coal balls in China. Higher Education Press, Beijing.

Winn AA 1999 The functional significance and fitness consequences of heterophylly. Int J Plant Sci 160(suppl):S113–S121.

Ziegler AM, G Eshel, P Rees, TA Rothfus, DB Rowley, D Sunderlin 2003 Tracing the tropics across land and sea: Permian to present. Lethaia 36:227–254.

This content downloaded from 147.188.216.059 on July 06, 2020 04:23:42 AM
All use subject to University of Chicago Press Terms and Conditions (http://www.journals.uchicago.edu/t-and-c).